
Since January 2020 Elsevier has created a COVID-19 resource centre with free information in English and Mandarin on the novel coronavirus COVID-19. The COVID-19 resource centre is hosted on Elsevier Connect, the company's public news and information website.

Chapter 16

# Eye and Associated Glands

**Dale G. Dunn**[1], **Julia F.M. Baker**[2] **and Steven D. Sorden**[3]

[1]*Covance Laboratories, Inc., Chantilly, VA, USA,* [2]*Charles River Laboratories, Inc., Frederick, MD, USA,* [3]*Covance Laboratories, Inc., Madison, WI, USA*

## Chapter Outline



**Boorman's Pathology of the Rat. DOI:** http://dx.doi.org/10.1016/B978-0-12-391448-4.00016-2

# 1. INTRODUCTION

The eye is susceptible to adverse toxic effects by direct application, inadvertent ocular contact, or systemic exposure to chemicals or their metabolites. Adverse ocular effects in humans have received considerable attention and evaluations for chemically induced ocular toxicity are commonly performed, but usually in species other than rodents. The albino rat is a less than ideal model for retinal toxicity because of the problems encountered with phototoxic retinopathy, the lack of pigment within the pigment epithelial layer, and a relatively high incidence of spontaneous retinal lesions. However, rodents have become popular in the study of glaucoma because of their ready availability, relative low cost, short life spans, and amenability to experimental and genetic manipulation. Toxicity and carcinogenicity studies in rats typically include the microscopic examination of a single histological section of each eye. This can only be considered a screening procedure for overt ocular toxicity. When a chemical is considered likely to have ocular toxicity, additional evaluations in other species should be considered.

# 2. NORMAL EYE AND ASSOCIATED GLANDS

## 2.1. Embryology

### *2.1.1. Eye*

The eye develops primarily from neuroectoderm and ectoderm. Most craniofacial mesenchymal tissue arises from neural crest cells. Consequently, with respect to the eye, mesoderm most likely gives rise only to the extraocular muscles and vascular endothelium.

Eye development begins when the optic vesicles form as lateral diverticula from the neural tube ectoderm of the forebrain on day 11 of gestation. As the vesicle approaches the surface ectoderm, it involutes to form the optic cup. The inner (inverted) layer of the optic cup will develop into the retina, the nonpigmented ciliary epithelium, and the posterior iris epithelium, whereas the outer layer becomes the retinal pigment epithelium (RPE), the pigmented ciliary epithelium, and the anterior iris epithelium. Contact of the optic vesicle with the surface ectoderm stimulates the formation of the lens placode, which invaginates to form the lens vesicle. By day 14, the lens vesicle has separated from the surface ectoderm and remains in the optic cup. In the separated lens vesicle, the posterior epithelial cells differentiate and elongate to become primary fibers, leaving epithelium only on the anterior surface. From these anterior epithelial cells, secondary fibers develop continuously over the lifetime of the rat (Figure 16.1).

By day 14, axons present in the inner layer of the retina invade the optic stalk, and by day 16, the optic nerve is grossly visible. The arachnoidal plexus, consisting of numerous blood vessels around the optic nerve, develops during the first postnatal week. The dura mater appears at this time as immature mesenchymal cells around the optic nerve (Figure 16.2).

All adult layers of the retina are present by day 8 after birth. Although melanosomes form in the pigment epithelium of the fetus, they disappear several weeks after birth in albino rats. Along with the pigment epithelium, the adult retina is composed of several different types of neurons (photoreceptors, horizontal, bipolar, amacrine, and ganglion cells)

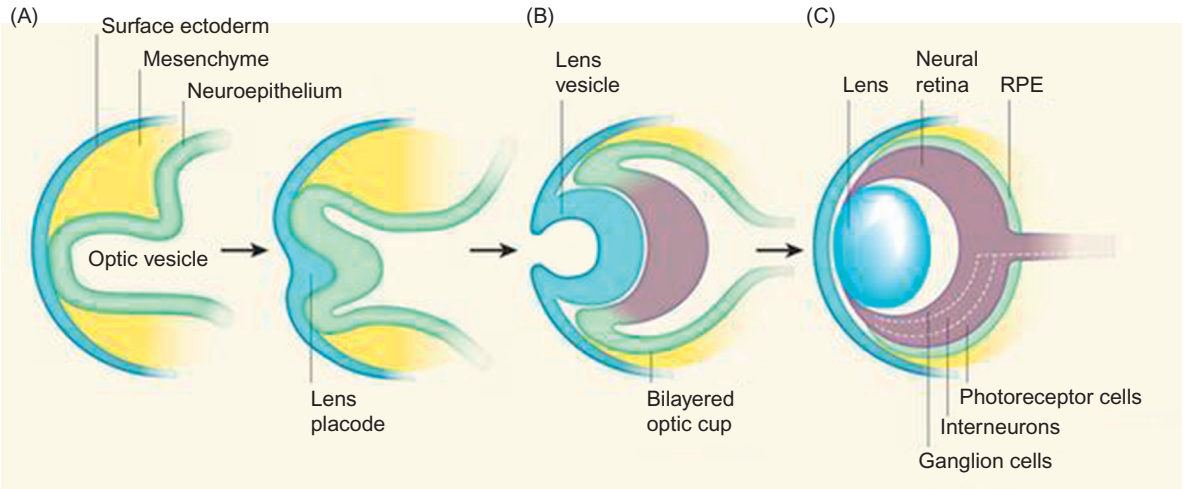


**FIGURE 16.1** Eye development. (A) At early stages of eye development, the surface ectoderm thickens and invaginates together with the underlying neuroepithelium of the optic vesicle. (B) The inner layer of the bilayered optic cup gives rise to neural retina and the outer layer gives rise to the retinal pigmented epithelium (RPE). (C) The mature neural retina comprises three cellular layers: photoreceptors, interneurons (horizontal, amacrine, and bipolar cells), and retinal ganglion cells. *Ali and Sowden (2011); reprinted by permission of Elsevier.*

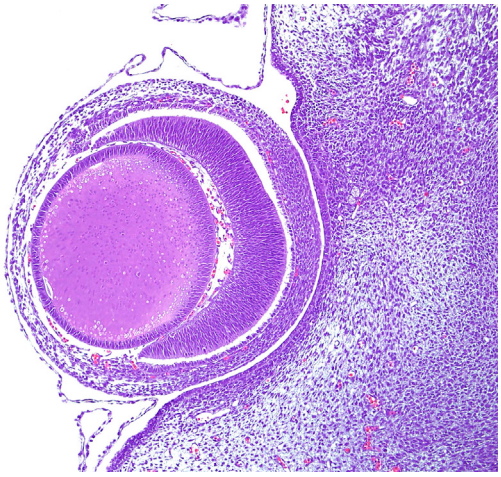

FIGURE 16.2 Histological section of a developing rat eye at day 15 of gestation.

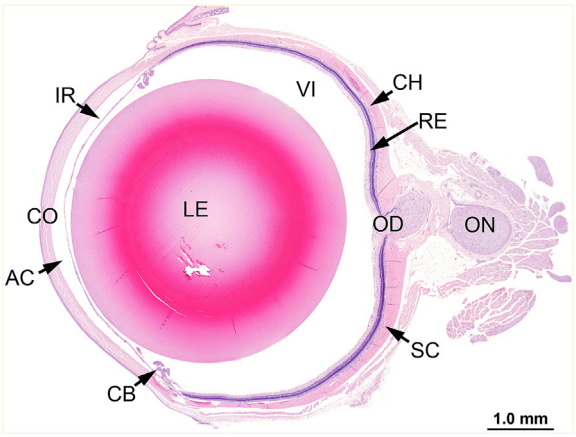


FIGURE 16.3 Histological section of a normal eye from a female F344 rat: cornea (CO), anterior chamber (AC), lens (LE), ciliary body (CB), iris (IR), choroid (CH), retina (RE), vitreous (VI), optic disk (papilla) (OD), and optic nerve (ON). *Image courtesy of the U.S. National Toxicology Program.*

and one type of specialized glial cell (Müller) organized into three distinct cellular layers. The neuronal cells and the Müller glia arise from a common pool of multipotent retinal progenitor cells. The sequence of development of these cell types is well conserved across the vertebrate species. Although there is considerable overlap in the production of retinal cell types at any time point, during embryogenesis, ganglion cells are generated first, followed by cone photoreceptors, horizontal cells, and most of the amacrine cells. Generated postnatally are the bipolar neurons, Müller glia, the remaining amacrine neurons, and most rod photoreceptors. The retina also contains astrocytes, endothelial cells, and microglia; however, these arise from separate lineages.

Infiltration of blood vessels and mesenchyme into the optic cup form the primary vitreous and tunica vasculosa lentis of the developing fetus. This hyaloid vasculature supplies the vitreous body and fetal lens. These vessels persist for the first days of life and normally regress in rats, via capillary apoptosis, between 10 and 20 days after birth. The eyes grow in proportion to age and brain weight, independent of body weight.

### 2.1.2. Adnexa

The lacrimal glands, including the Harderian gland, develop from solid cords of undifferentiated cells that invaginate from the surface ectoderm on day 19 of gestation. Pigment is first seen in the Harderian gland acini by day 9 after birth.

## 2.2. Anatomy and Histology

### 2.2.1. Eye

The eye of the rat is nearly spherical, 5–6 mm in diameter, and weighs 110–145 mg at 18 weeks of age. The neonatal rat is born with its eyes closed and an immature visual system that has been compared to that of the human fetus at 26 weeks of gestation. The visual system of the newborn rat gradually matures from birth, the first manifestation being the opening of the eyes, which usually takes place at postnatal day 14. Maturation of the retina and visual pathways is normally complete by the end of the first month (Figure 16.3).

The outer fibrous tunic of the eye consists of the cornea and sclera. The cornea has an external nonkeratinized, stratified squamous epithelium overlying a basement membrane; a stroma composed of lamellae of collagen fibers, keratocytes, and myofibroblasts; Descemet's membrane; and an internal endothelium. The stroma and endothelium are neural crest derivatives. The surface of the corneal epithelium is covered by fine microvilli. The cornea does not contain blood vessels and Bowman's membrane, as defined in humans, is not present in the rat (Figures 16.4 and 16.5).

The uvea, which provides the vascular supply to almost all intraocular tissues, consists of the iris, ciliary body, and choroid. The iris arises from the anterior portion of the ciliary body and is the anterior continuation of the choroid. The iris is completely devoid of pigment in the albino rat and consists primarily of loose, highly vascular connective tissue. The anterior surface is covered by endothelial cells, which are reflected from the posterior lining of the cornea. The posterior surface is covered by a bilayered epithelium similar to that of the ciliary body. The ciliary body, situated between the root of the iris and the anterior termination of the choroid, is covered by two layers of epithelial cells. Microfibrils arising from the basement membrane of the inner ciliary epithelium and extending to the lens capsule form the ciliary zonule or

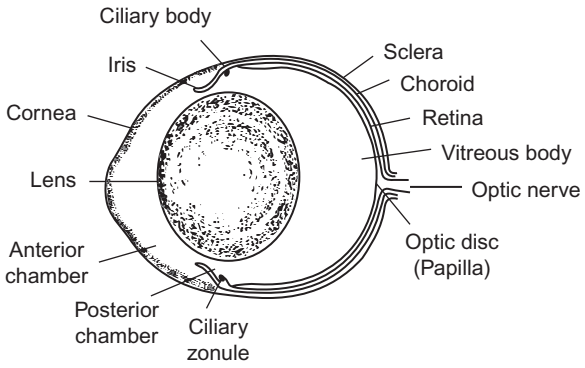


**FIGURE 16.4** Schematic drawing of the rat eye.


**FIGURE 16.5** The cornea is covered by epithelium (E), which is separated from the stroma (S) by a thick basement membrane (arrow). Descemet's membrane (D) is the homogenous lamella on the inner surface of the stroma covered by a thin endothelium.

suspensory ligament. The ciliary muscle in the rat is poorly developed. The choroid, situated between the sclera and the pigment epithelial layer of the retina, consists of connective tissue, capillaries, and melanocytes in pigmented species. Rodents typically do not have a tapetum lucidum and this is true for the rat. However, a vestigial tapetum, identified only as an area of decreased melanosomes in the superior retina, may be present in Long–Evans rats.

The components of the mammalian retina are well established. The classic view of a retina based on a 6 to 12 cell module has been replaced by a more complex model characterized by multiple parallel arrays containing five major classes of neurons and at least 60 functionally different cell types. Although the vast majority of these cell types cannot be distinguished by routine light microscopy, a brief summary is included here for its potential relevance to the pathophysiology and/or pathogenesis of spontaneous and toxicological lesions.

The principal cell types of the retina are the pigment epithelium, rod and cone photoreceptors, horizontal cells, bipolar cells, amacrine cells, Müller glial cells, and ganglion cells, which are organized into three distinct cellular layers. The rat, like most nocturnal animals, does not have areas of increased visual acuity like the macula and fovea.

The cells of the RPE sit on Bruch's membrane, a trilayered structure composed of the basement membrane of the RPE, an elastic-collagen layer, and a component of the endothelial basal lamina of the subjacent choriocapillaris. This microanatomic arrangement is well preserved across species. The pigment epithelium consists of cuboidal to columnar cells with basal nuclei and cylindrical sheaths on the apical surface that invest the tips of the rod and cone photoreceptor cells. The pigment cells play an important role in the visual cycle by processing vitamin A into 11-cis-retinal, the molecule necessary for visual pigment regeneration in the photoreceptor cells.

Each photoreceptor cell has a dendrite that assumes the form of a rod or cone (photoreceptor layer) and contains numerous flattened membranous vesicles; the visual pigment is located on the outer surface of the lipid bilayer of the vesicles. The pole opposite the dendrite synapses with bipolar neurons. The generic mammalian retina contains one type of rod photoreceptor and two types of cone photoreceptors. One type of cone photoreceptor is sensitive to short and the other to long wavelengths of light. A comparison of the outputs of the two types of cone photoreceptor cells provides the basis for color vision. The predominant photoreceptor cells in the rat are rods. The nuclei of the rod and cone photoreceptor cells form the outer nuclear layer.

The nuclei of the bipolar, horizontal, amacrine, and Müller glial cells make up the inner nuclear layer. The proportions of horizontal, bipolar, and amacrine cells are similar across mammalian species. The mammalian retina contains a single type of rod-associated bipolar cell and a dozen different types that receive their input from cones. Specific types of bipolar cells synapse on specific types of ganglion cells. Most mammals have two types of horizontal cells. The first type (type A) has a simple dendritic arbor that connects with the axonal terminals of the cones. The second type (type B)—and the only type present in rats, mice, and gerbils—has two dendritic arbors, one associated with cones and one with rods. Amacrine cells, with at least 29 different varieties, are the most diverse type of retinal neuron and their functions are apparently as varied as their forms.

Ganglion cells have dendrites that synapse with bipolar cells and axons that combine to form the optic nerve. Ganglion cells vary more in their morphology from species to species than any other retinal cell type. Mammalian retinas are believed to contain at least 20 different types of ganglion cells. The discovery of an intrinsically photoreceptive ganglion cell has dramatically

altered the longstanding view that phototransduction occurs only in rods and cones. These novel ganglion cells express the photopigment melanopsin and are divided into several subtypes.

Retinal neurons are spaced such that neurons of the same type maintain a minimum distance from each other. Supporting cells of the retina include neuroglia and Müller cells; the terminal expansions of Müller cells constitute the inner and outer limiting membranes. Although the rodent optic nerve head (papilla, disk) has a poorly developed collagenous lamina cribrosa, it has some anatomic features in common with primates. Consequently, models of chronically elevated intraocular pressure in rats and mice have proven increasingly useful (Figure 16.6).

The lens is an avascular, transparent, biconvex spherical body occupying about two-thirds of the intraocular cavity. It consists of laminated fibers formed by modified epithelial cells and enclosed by a capsule. A simple cuboidal epithelium is present beneath the capsule on the anterior and equatorial surfaces. The cells at the anterior pole are relatively inactive. Lens epithelial cells in the germinative zone of the peripheral equatorial region undergo mitosis, and their progeny are displaced posteriorly into the transitional zone, where they begin to differentiate into cortical fiber cells of the lens substance, a process regulated by a fibroblast growth factor gradient. Fiber differentiation results in distinct molecular and morphologic changes, e.g., exit from the cell cycle, elongation, loss of cytoplasmic organelles and nuclei, and accumulation of crystallin proteins. The proteins of the lens are typically organ and species specific. The nuclear bow comprises remnants of nuclei that are lost in the process of fiber formation. The tips of the differentiating fibers eventually join to form the anterior and posterior suture lines visible by slit-lamp biomicroscopy. Because the small diameter of the globe necessitates a high dioptric power of the lens, the size of the lens relative to that of the eye is remarkably large in rats compared to humans. The rat is believed to be unable to accommodate; nocturnal and with relatively poor visual abilities, rats have little need for accommodation (Figure 16.7).

The mammalian vitreous body is a transparent gelatinous substance situated between, and providing support and protection to, the lens and the retina. It consists of approximately 99% water but has a viscoelastic and gelatinous nature because of the presence of collagen and uronic acid-containing polyanionic macromolecules (i.e., hyaluronan, versican, and collagen IX). Hyaluronan, the principal uronic acid-containing molecule, is associated with water molecules and dispersed between strands of collagen fibers, producing a cross-linked polymer network. Viscosity of the vitreous is increased behind the lens compared to the region closest to the retina because of a higher concentration of hyaluronan at this site. Likewise, rigidity is increased around the perimeter because of a predominance of collagen. Hyalocytes, bone-marrow-derived tissue macrophages, are found in the peripheral or cortical region of the vitreous body adjacent to the retina. Hyalocytes are concentrated anteriorly in the vitreous base (the zone of strongest attachment near the ora ciliaris retinae) and posteriorly near the optic papilla.

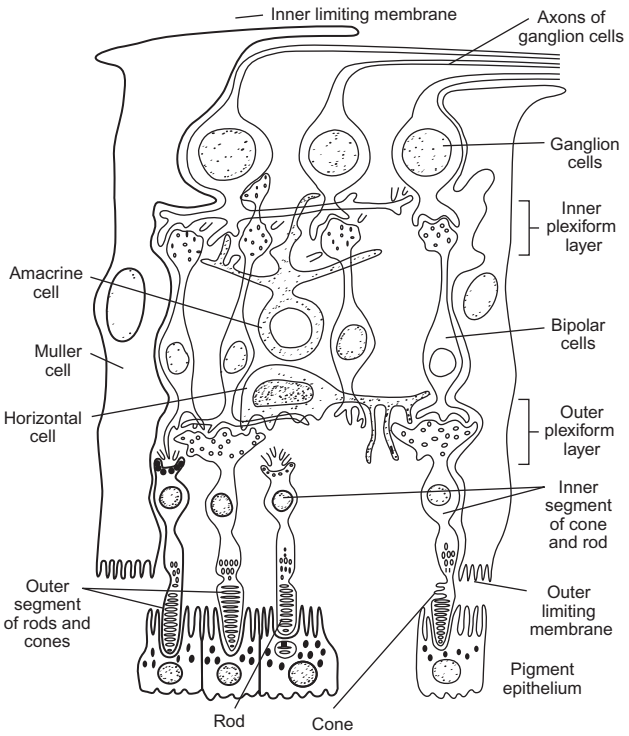


**FIGURE 16.6** Schematic drawing of the retina showing the various layers.

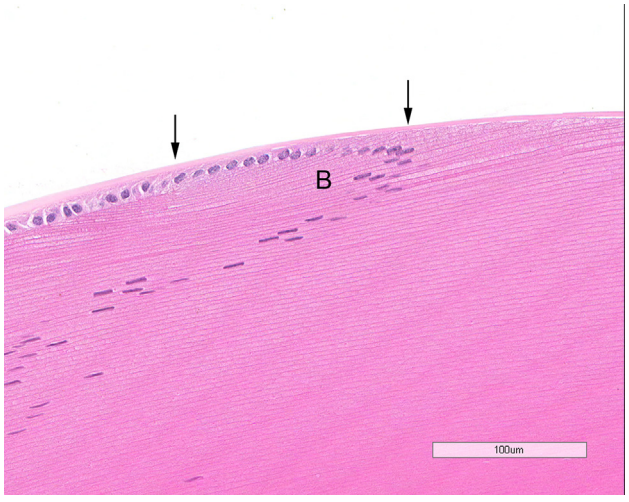


**FIGURE 16.7** The lens epithelial cells become elongated in the bow area (B) and are transformed into lens fibers. Lens capsule (arrows).

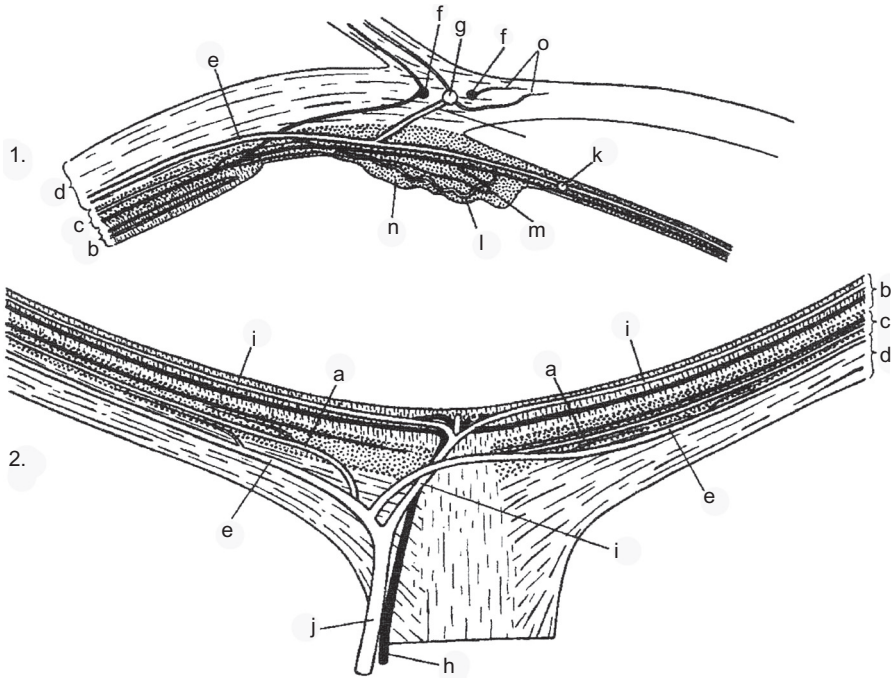


**FIGURE 16.8** 1. Diagram of the blood vessels of the anterior segment of the rat eye. 2. Diagram showing distribution of blood vessels in the posterior segment of the eye. (a) Short posterior ciliary artery. (b) Retina. (c) Choroid. (d) Sclera. (e) Long posterior ciliary artery. (f) Corneoscleral veins. (g) Corneoscleral artery. (h) Retinal vein. (i) Retinal artery. (j) Ophthalmic artery. (k) Major arterial circle. (l) Ciliary artery. (m) Ciliary vein. (n) Ciliary body. (o) Marginal corneal vessels. *Janes and Bounds (1955); reprinted by permission of Wiley.*

The intraocular branch of the ophthalmic artery, lying in the inferior-nasal quadrant of the optic nerve sheath, supplies most of the blood reaching the rat eye. This vessel gives rise to the central retinal artery and ciliary arteries. The central retinal artery continues forward between optic nerve fibers to emerge over the optic papilla. From there, as in other species with a holangiotic vascular pattern, symmetrically arranged retinal arteries (approximately six) radiate to the equator, supplying two layers of capillaries to the inner retina: one in the outer plexiform layer and one in the inner plexiform layer. The choroid is supplied by branches from two long posterior ciliary arteries, one nasal and one temporal, and several short posterior ciliary arteries. These vessels form arterioles and capillaries (choriocapillaris) directly beneath the Bruch's membrane. The choroidal circulation nourishes the outer retina (RPE and photoreceptor cells). Anteriorly, the main ciliary vessels divide dichotomously and form the major arterial circle of the iris. The major arterial circle gives rises to arteries supplying the iris and ciliary body. In the region of the ciliary body, and prior to the formation of the major arterial circle, each long posterior ciliary artery communicates with the arterial component of the corneoscleral vascular circle. This limbal vascular plexus is also supplied externally by the anterior ciliary arteries, providing a potential collateral blood supply to the anterior segment analogous to that of primates. Blood is drained from the eye chiefly by four vortex veins, located just posterior to the equator on the dorsal, ventral, nasal, and temporal sides. The central retinal vein drains the retina (Figure 16.8).

The rat anterior segment receives sensory innervation from the ophthalmic nerve, the first branch of the trigeminal nerve. Cell bodies for these sensory nerves are located in the trigeminal ganglion. Sensory nerve endings lie in the cornea, iris, and ciliary body. Sympathetic nerve fibers reach the eye by many pathways, e.g., ophthalmic, oculomotor, and abducens nerves. Rat anterior segment sympathetic innervation mainly derives from the superior cervical ganglion. Most sympathetic nerve fibers reach the iris and ciliary body by way of the base of the ciliary body. There is dense innervation of the iris with nerve endings in the dilator and sphincter muscles, and adjacent to blood vessels.

### 2.2.2. Adnexa

The outer surface of the eyelid contains hair and associated sebaceous glands. Approximately 12–15 branched sebaceous glands (meibomian or tarsal glands) are located on the inner margin of the lids. The third eyelid located in the nasal angle of the palpebral fissure consists of a connective tissue stroma supported by hyaline cartilage. The conjunctiva extends from the margin of the eyelid to the anterior segment of the globe at the limbus (Figure 16.9).

In the rat, the Harderian gland is large, covering seven-eighths of the deep bulbar circumference. Highly irregular in shape, it is unified medially and subdivided laterally by three clefts, through which pass the optic nerve and several extraocular muscles. It closely apposes the orbital venous sinus. The gland weighs 290–360 mg


FIGURE 16.9 The outer surface of the eyelids contains the sebaceous glands of Zeis (Z), whereas the inner surface contains the meibomian (tarsal) glands (M).

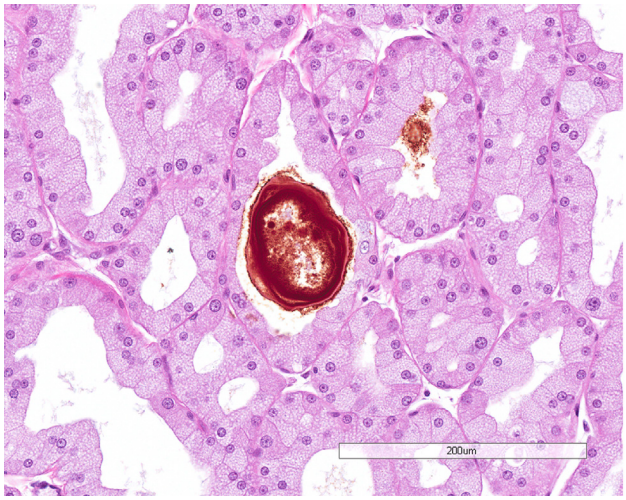


FIGURE 16.10 Harderian gland with alveoli composed of finely vacuolated epithelium; note laminated concretion in lumen.

(0.07−0.08% of body weight) in 18 week old rats. A single excretory duct originates at the hilus and opens on the outer (nasal) side of the third eyelid. The gland is a branched tubuloalveolar gland without distinct intralobular ducts. Alveoli are lined by columnar cells with numerous clear cytoplasmic vacuoles and round basal nuclei; the alveolar lumina appear empty or contain yellow-brown wispy strands or laminated concretions of porphyrin secretion. Two types of secretory cells are distinguishable based on size and shape of secretory granules. Type A cells are more numerous and contain large secretory vacuoles, whereas type B cells contain abundant mitochondria and packets of smooth endoplasmic reticulum. Flattened myoepithelial cells are situated between the secretory cells and the basal lamina surrounding the alveoli, but are not easily distinguished in histological sections. The secretory product of the Harderian gland consists primarily of lipids (wax esters), which are released into the lumen by the process of exocytosis (merocrine-type secretion); the Harderian gland is the only mammalian gland known to secrete lipid by this method. Epithelial cells also produce and secrete porphyrin. The production of indoleamines is a function the Harderian gland shares with the pineal gland and retina. Of the major head and neck glands of the rat, the Harderian gland has the highest density of lymphatics (Figure 16.10).

The rat has two pairs of lacrimal glands. The extraorbital (exorbital) gland, anterior to the parotid salivary gland, is slightly flattened, bean-shaped, and weighs 175−205 mg in 18-week old rats. The triangular intraorbital gland is located near the posterior lateral border of the Harderian gland between the zygomatic arch and the eye; it weighs 20−40 mg.

The extraorbital gland has four or five excretory ducts, which fuse to form two or three main ducts. The main ducts fuse with the two ducts from the intraorbital gland to form a common duct before entering the conjunctival sac. The lacrimal ducts begin lateral to the nasal angle of the palpebral fissure (puncta lacrimalia) and fuse to form the nasolacrimal duct, which opens ventromedially into the nasal vestibule at the anterior end of the maxilloturbinate.

The lacrimal glands are lobulated and consist of serous acini with narrow lumina and a branching duct system of intralobular (intercalated) ducts similar to those of the salivary glands, interlobular ducts, and excretory ducts. Acinar cells are polyhedral or pyramidal with round to oval nuclei; some acinar cells are enlarged and contain hyperchromatic nuclei two to four times the size of the typical nucleus (cytomegaly and karyomegaly). These are more prominent in males than females and become more frequent with age. Acini in males are generally larger than in females (Figure 16.11).

## 2.3. Physiology

### *2.3.1. Eye*

Normal function of the eye is dependent on the transparency and refractivity of the cornea and lens, the reception and transduction of light stimuli by the retina, and the transmission of these signals in the form of nerve impulses to the appropriate portions of the brain. The physiology of the eye is complex and there are numerous texts on the subject, but few deal specifically with the rat. A complete discussion of vision is beyond the scope of this chapter, but brief mention is made of factors

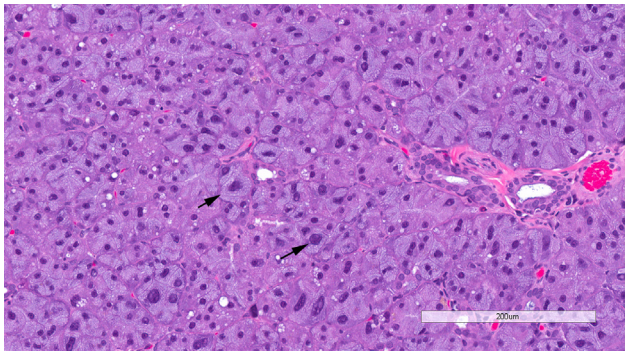

**FIGURE 16.11** Exorbital lacrimal gland showing cytomegaly and karyomegaly (arrows), which are common features in aging rats.

important in the pathophysiology of common spontaneous and toxicological lesions.

The eye is protected by the blood ocular barrier system: the blood–aqueous barrier and blood–retina barrier. The blood–aqueous barrier consists of the iridal endothelium, which prevents movements of macromolecules from the blood into the iridal stoma, and the ciliary and iridal epithelium, which protect the posterior chamber of the aqueous. Nonpolar lipid-soluble compounds can penetrate the blood–aqueous barrier, whereas highly polar compounds are generally excluded. The blood–retinal barrier is also composed of two parts, both of which comprise cells connected by tight junctions: the endothelium of the retinal vessels and the pigment epithelium.

Several adaptations enable the retinal vasculature to match blood flow to the retina's high metabolic demand. The retinal vasculature consists exclusively of microvessels (arterioles and capillaries). Retinal capillaries have a high density of pericytes, whose contractions are believed to regulate local perfusion by changing capillary diameter. The precapillary tertiary arteriole and its associated capillary network may constitute an operational unit, resulting in decentralized regulation of retinal blood flow. The retinal vasculature lacks autonomic innervation and is thus not subject to diminishment because of the metabolic needs of other tissues.

The epithelium and endothelium of the cornea are important in maintaining normal transparency: necrosis and loss of these cell layers results in imbibition of water and loss of clarity. The hypertonic tears and other secretions at the front of the cornea, along with the hypertonic aqueous at the back, maintain the cornea in a state of relative dehydration necessary for transparency. Inflammation in the cornea is also associated with an increase in water (as well as leukocytes); with severe inflammation, vascularization and fibrosis may result in permanent loss of transparency.

The transparency of the lens is dependent on the highly ordered arrangement, size, uniformity of shape and dimension, and molecular structure of the lens fibers. The primary function of lens metabolism is to maintain the organized structure and transparency. Interference with lens metabolism or active transport across cell membranes, breakage of the lens capsule, and other types of injury can alter the refractive index and optical properties of the lens, resulting in a cataract.

The lens uses glucose as its primary, and perhaps sole, source of energy. Most of the glucose is metabolized by glycolysis, because the lens functions in a low oxygen environment and has low levels of the enzymes associated with aerobic oxidation of glucose. Movement of water into and out of the lens occurs passively and is regulated by the transport of cations, primarily in the anterior epithelium. The energy for this transport is derived from the hydrolysis of ATP by $Na^+$, $K^+$-activated ATPase. The lens maintains a high internal concentration of potassium and a low concentration of sodium.

Because the lens has no blood supply, it depends on the aqueous humor for oxygen and nutrients. Aqueous humor flows between the anterior surface of the lens and the iris en route to the anterior chamber. Thus, the anterior surface of the lens near the equator may be exposed first, and to the highest concentration, to toxic chemicals, perhaps explaining why many toxic cataracts are first seen in this area. The amount of an exogenous substance or potential cataractogenic agent that the lens is exposed to is determined by physical–chemical interactions, as well as possible active transport of the substance into the aqueous humor.

As an ultrafiltrate of blood, the concentration of protein in the aqueous humor is much less than that of serum; thus, adsorption of an exogenous substance or drug to plasma protein retards its penetration into the aqueous humor. Also, the steady-state concentration of most small water-soluble molecules in aqueous humor is less than that in plasma as a result of molecular sieving. Penetration of molecules through the cell membrane of the ciliary epithelium increases with lipid solubility. Therefore, the rate of penetration of a substance into the aqueous humor and its steady-state concentration in the aqueous humor relative to that in plasma increase with increasing lipid solubility and decreasing molecular size.

Maintenance of intraocular pressure within physiological limits depends on a balance between production and outflow of aqueous humor. The ciliary processes produce the aqueous humor by a combination of diffusion, ultrafiltration of blood, and active secretion into the posterior chamber. The aqueous humor flows through the pupillary opening into the anterior chamber, where it enters the ciliary cleft via spaces within the pectinate ligament bridging the iridocorneal angle. Aqueous outflow continues through the collagenous framework of the ciliary cleft and the corneoscleral meshwork embedded in the sclera. The corneoscleral meshwork is closely associated with collector

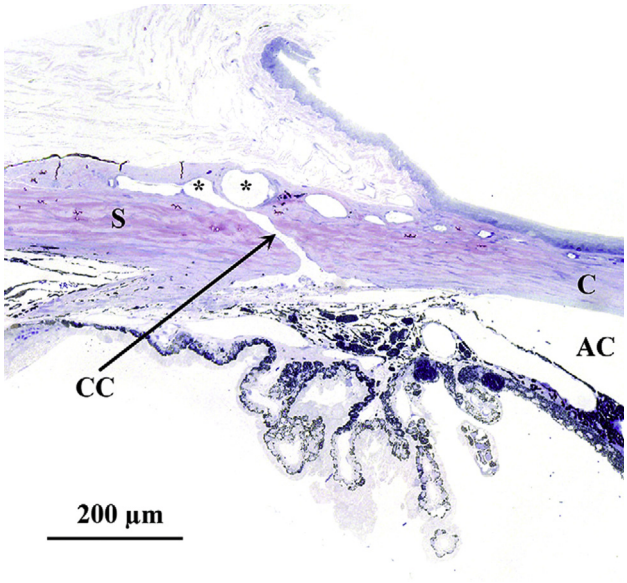


**FIGURE 16.12** Histological section through the limbus of a rat eye showing sites of experimental aqueous humor outflow obstruction. This section fortuitously demonstrates an aqueous collector channel (CC) traversing the limbal sclera and connecting Schlemm's canal with the limbal blood vessels (*): anterior chamber (AC), sclera (S) and cornea (C). *Morrison et al. (2011); reprinted by permission of Elsevier.*

vessels of the angular aqueous plexus, a structure analogous to the canal of Schlemm in primates. Relying on a pressure gradient, fluid is transported to the intrascleral venous plexus and then passes into the scleral and choroidal veins. An alternative uveoscleral route through the ciliary body interstitium to the suprachoroidal space and vortex veins accounts for a small percentage of aqueous escape (Figure 16.12).

The vitreous structure created by collagen and hyaluronan results in a diffusional barrier to macromolecules; however, small molecules diffuse freely. Small molecule composition and enzymatic activity (e.g., acetylcholinesterase) in the vitreous differ among species. In the rat, cysteine is consistently present; ascorbic acid is present at lower levels than in other species; and glutathione (GSH), uric acid, and tyrosine concentrations are higher than in other species. These electrochemically active components may function as antioxidants. Diet may affect the components of, and metabolites found within, the vitreous. Hyalocytes, the bone-marrow-derived tissue macrophages found at the periphery of the vitreous, inhibit proliferation of endothelial cells and the RPE.

Phototransduction and the visual process begins when light passing through the cornea and lens, reaches the retina, and is absorbed by visual pigments of the rods (rhodopsin) and cones (cone opsins). The visual pigments are integral membrane bound proteins attached to the highly light-sensitive chromophore, 11-cis-retinal. Capture of light results in the isomerization of 11-cis-retinal to all-trans-retinal, the formation of photoactive visual pigment, and activation of the transduction cascade. Bleaching of the visual pigment increases the calcium conductance of the vesicular membranes and promotes the diffusion of calcium to the intracellular space, where it acts on the cell membrane, reducing its permeability to sodium and promoting hyperpolarization. The signal generated is transmitted to the bipolar cells and then the ganglion cells, which create action potentials along their axons and relay the information to the central nervous system. Horizontal cells receive an excitatory synaptic input from the cones and make an inhibitory output back onto the cones. Amacrine cells receive a direct excitatory input from bipolar cells and make inhibitory inputs back onto the axon terminals of the bipolar cells. Each of the different types of ganglion cell is believed to relay different aspects of the visual scene to the brain.

Sustained phototransduction requires the continuous replacement of 11-cis-retinal through a process known as the visual cycle. This is largely accomplished by cycling of vitamin A analogs between the photoreceptor cells and the RPE, a major site of synthesis of 11-cis-retinal from all-trans-retinol (vitamin A). The apical aspect of pigment epithelial cells is closely associated with the photoreceptor outer segments. Microvilli on the surface of the pigment epithelium invest and phagocytose the distal tip of the photoreceptor outer segments. These internalized disks contain the molecules that are recycled and subsequently redelivered to the photoreceptor cells. The RPE also transfers to the photoreceptor cells essential nutrients (e.g., glucose, vitamin A, docosahexaenoic acid) from the choroidal circulation. Cone pigment replacement is not as well understood, but is known to include an alternate pathway separate from the RPE involving the Müller glial cells. The proximal portions of photoreceptor outer segments are synthesized daily by cell bodies and outer segment tips are shed with a circadian rhythm. The process results in a complete turnover of outer segments about every 9 days.

The intrinsically photoreceptive retinal ganglion cells, which express melanopsin, are obligatory for several nonimage-forming visual activities, including circadian photoentrainment and pupillary light reflexes. Glial cells (Müller cells and astrocytes) maintain retinal fluid homeostasis in part through aquaporin water channels.

### 2.3.2. Adnexa

The lacrimal glands secrete tears, which hydrate the cornea, clean the entire conjunctival sac and superficial cornea, and supply nutrition to the corneal and conjunctival epithelium. The aqueous component of the tear film is responsible for keeping the cornea buffered, lubricated,

nourished and protected and is produced and secreted from the main and accessory lacrimal glands. The exorbital gland is the main lacrimal gland of the rat and is analogous to the human lacrimal gland. About 80% of the normal lacrimal gland consists of serous acini that secrete protein, electrolytes, and water. The major protein secreted from the lacrimal acini is lipocalin; other secreted proteins include lysozyme, peroxidase, lactoferrin, beta lysine, and secretory immunoglobulins A and G. The exorbital lacrimal gland provides 99% of the immunoglobulin A present in the tears coming from the lacrimal glands. Proteins in tears, which may act as surfactants, decline with age in rats; 24-month-old rats have only 65% as much protein as 4-month-old rats.

Various functions have been ascribed to the mammalian Harderian gland. The primary purpose may well be to contribute to the secretions at the front of the eye. Among other possible roles, the Harderian gland has been held to be a site of immune responses, a photoprotective organ, a source of pheromones, and part of the retinal−pineal axis. Plasma cells reside in the interstitium of the rat Harderian gland. Porphyrin content decreases in the rodent Harderian gland, while increasing in the conjunctival sac, in response to a rapid increase in light intensity, suggesting a photoprotective role (protoporphyrin is capable of transducing light in the UV range into the visual red). By absorbing UV light, porphyrins may also protect antigen-presenting cells. Sex steroids affect porphyrin levels, and secretions of the Harderian gland may act as pheromones. The Harderian gland may also act as an extraretinal photoreceptor, affecting pineal serotonin levels, and may influence the development of the visual cortex in the neonatal rat. The Harderian gland is one of the nonpineal sources of melatonin.

## 3. CONGENITAL LESIONS

A variety of congenital ocular disorders is described in the rat, some of which occur commonly. Although several experimental models of microphthalmia exist, the condition also occurs spontaneously. In the Fischer 344 (F344) rat, microphthalmia occurs with considerable frequency, more commonly in females than males and in the left eye more often than the right. Congenital anophthalmia has been reported in the rat, but generally in specifically anophthalmic strains. Corneal inclusion cysts have been reported to occur as congenital lesions or following trauma. Corneal dermoid in the rat is exceedingly rare. Cataracts may occur congenitally in Sprague−Dawley and F344 rats, as well as in aging animals.

Anomalies of the fetal ocular vasculature are common in rats and include persistent pupillary membrane, persistence of hyaloid vasculature, and preretinal loops and saccular aneurysms of the retinal vessels. Persistent pupillary membranes are occasionally observed, but the frequency decreases with increasing age. The pupillary membranes are remnants of the iris, which completely covers the fetal lens; pupillary membranes usually regress by birth. Persistent membranes are recognized clinically as multiple strands of tissues crossing the pupillary opening, but are not usually seen in routine histological preparations. Adherence of the pupillary membrane to the anterior surface of the lens may cause a focal opacity or a cataract. Remnants of the hyaloid vessels, which usually regress, are infrequently seen in aging rats. Persistent hyperplastic primary vitreous is rare. Tortuosity of retinal vessels and preretinal arteriolar loops have been noted as common retinal abnormalities in rats.

Coloboma is an outpouching of neuroectoderm due to incomplete closure of the embryonic fissure in the floor of the optic cup and stalk. Optic disk coloboma occurs relatively commonly and may be associated with microphthalmia or iridal coloboma. Coloboma of the iris is uncommon and has been reported with coloboma of the choroid and optic nerve. Coloboma of the choroid without involvement of the optic nerve also occurs.

Retinal folds or rosette-like formations are common in rats; they may be congenital, but may also result from focal retinal separation. Retinal separation, whether spontaneous or congenital, is rarely seen in rats. Retinal degeneration may be seen as an inherited defect or environmentally induced lesion (Figure 16.13).

Complete optic nerve hypoplasia or aplasia is also seen as a congenital defect. Optic nerve abnormalities described as dysplasia (nodular thickening, curvature, bifurcation) and associated with a meningeal defect have been observed in young Sprague−Dawley rats.

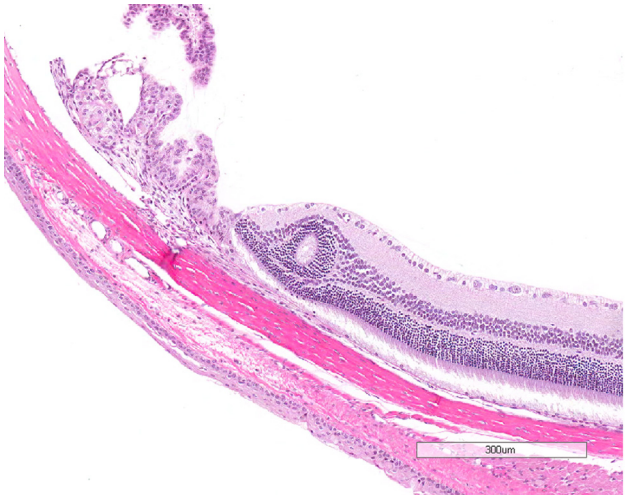


**FIGURE 16.13** Histological section of retinal rosette.

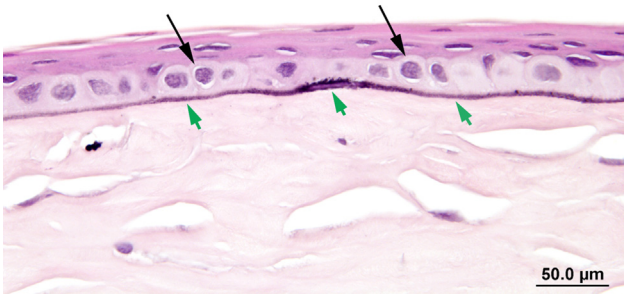


FIGURE 16.14 Minimal linear corneal mineralization (green arrows) within and subjacent to the epithelial basement membrane. There is diffuse thinning of the overlying corneal epithelium and swelling of the corneal epithelial basal cells (black arrows). *Image courtesy of the U.S. National Toxicology Program.*

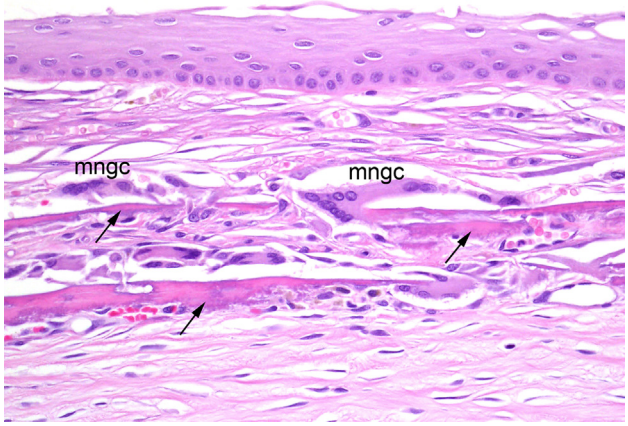


FIGURE 16.15 Cornea with mineralization (arrows) deeper in the corneal stroma. Minimal secondary granulomatous inflammation is present (note multinucleated giant cells (mngc) adjacent to a mineralized plaque). *Image courtesy of the U.S. National Toxicology Program.*

# 4. DEGENERATIVE LESIONS

## 4.1. Eye

### *4.1.1. Corneal Mineral Deposits*

Calcium is present close to saturation levels in the corneal stroma, and minimal increases in blood calcium levels may cause precipitation; even desiccation of the cornea due to proptosis or anesthesia may lead to the formation of mineral deposits.

Small deposits of mineral in the cornea may be detected as opacities on ophthalmic examination in many strains of rat, including the Fischer, Sprague–Dawley, Wistar, and Long–Evans. The incidence of this condition tends to increase with age; in Sprague–Dawley rats, the condition is uncommon (<1%) in young animals, but rises to 25% in males and 10% in females at 110 weeks of age. Microscopically, these lesions correlate with basophilic granularity in the region of the stromal–epithelial interface, occasionally associated with mild proliferation of spindle-shaped cells in the surrounding stroma. More rarely, the mineral may be associated with Descemet's membrane. This mineral deposition is frequently referred to as corneal dystrophy by clinicians. No other evidence of ocular disease is seen and it is important to distinguish this condition from dysplastic mineralization secondary to keratopathies with inflammation and necrosis. Mineral deposition has also been reported in association with ketamine–xylazine anesthesia in young rats (Figures 16.14 and 16.15).

### *4.1.2. Scleral Osseous/Cartilaginous Metaplasia*

Characterized by single to multiple plaque-like deposits of cartilage or well-differentiated mineralized bone,

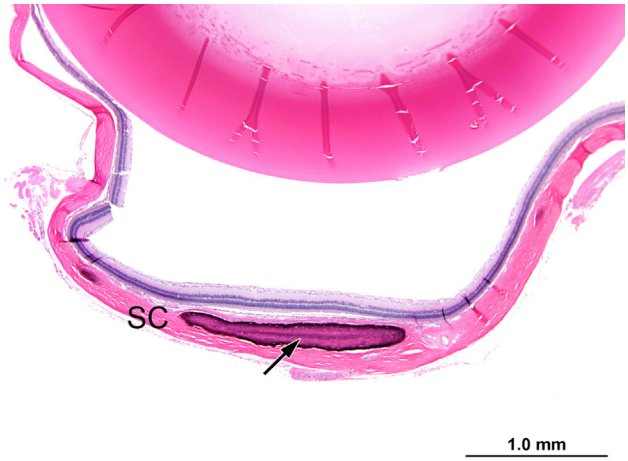


FIGURE 16.16 Osseous metaplasia of the sclera (arrow). Adjacent ocular tissues are unremarkable. *Image courtesy of the U.S. National Toxicology Program.*

osseous/cartilaginous metaplasia of the sclera occurs commonly in aging F344 rats. The condition resembles the senile hyaline scleral plaques seen in humans and adjacent ocular tissues are unremarkable. This change is seen less frequently in other strains of rat (Figure 16.16).

### *4.1.3. Cataracts*

The lens and retina are the most common sites of degenerative changes in the eye. The density of the lens nucleus is related to the concentration of insoluble proteins. In the young rat, lens proteins are largely soluble and the lens absorbs little UV radiation; indeed, the absorption spectrum in the eye of juvenile rats resembles that of the aphakic eye. In the aging rat, there is an increase in the

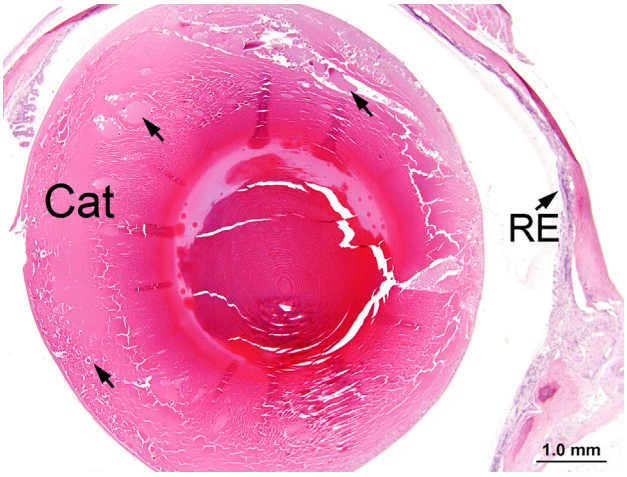


FIGURE 16.17 Lens exhibits cortical cataract (Cat) characterized by swelling and disruption of lens fibers (arrows). The retina exhibits atrophy/degeneration. *Image courtesy of the U.S. National Toxicology Program.*

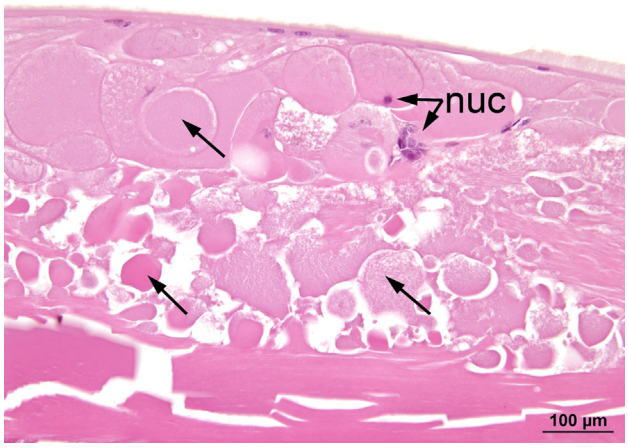


FIGURE 16.18 Lens fibers (arrows) in a cataractous lens exhibit various abnormal features including separation, swelling, granularity, condensation, fragmentation, and loss of normal orderly configuration. Note the abnormal retention of lens fiber nuclei (nuc) in several swollen lens fibers. *Image courtesy of the U.S. National Toxicology Program.*

concentration of insoluble proteins and a decrease in soluble proteins, resulting in increased density of the nucleus. Increased nuclear density results in optical discontinuity between the cortical region and the nucleus, recognizable on slit-lamp biomicroscopy. Lens fibers within the aged nucleus show decreased affinity for eosin compared to the cortical fibers, resulting in a pale lens center in hematoxylin- and eosin-stained sections. Other age-related changes in the rat lens include the development of small vacuoles associated with the anterior and posterior suture lines and the presence of irregularly swollen lens fibers with finely granular cytoplasm in the anterior cortex—recognized as segmental striations originating in the periphery and forming an arcuate pattern on slit-lamp examination.

Any alteration that results in opacity of the lens may be classified as a cataract. Such lesions may be unilateral or bilateral and may involve the capsule, the anterior or posterior cortex, or the nucleus. Any factor that causes scattering of light during its passage through the lens will result in opacity; such factors include disruption of the lens epithelium, irregular enlargement of lens fibers, granular or liquefactive degeneration of lens fibers, and mineral deposition. Large ovoid or round cells (balloon cells) may be evident adjacent to degenerate lens fibers and may or may not include nuclei in the plane of section. Nuclei situated in the region of the nuclear bow become disorganized and start to migrate toward the center of the lens, whereas equatorial epithelial cells migrate toward the posterior pole. As cataracts mature, there is destruction of the cortex, frequently accompanied by progressive mineralization of the debris. Lens epithelial cells may be lost or undergo fibrous metaplasia. With the loss of the normal cortical structure, the capsule becomes distorted and may show adhesion to the iris or ciliary body (posterior synechia formation) (Figures 16.17-16.23).

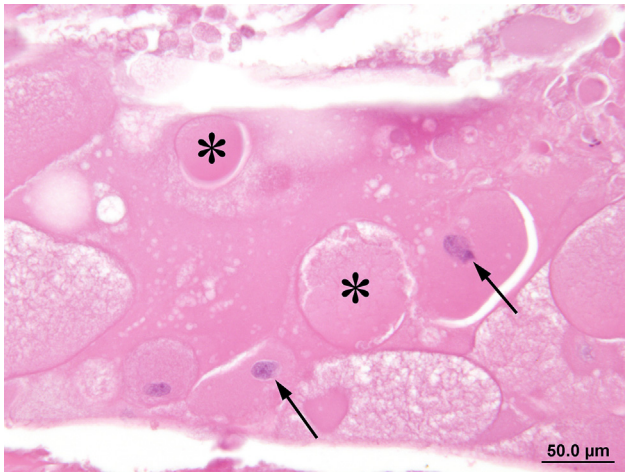


FIGURE 16.19 Rounded, swollen fibers in a cataract are sometimes called Morgagnian globules (*). Swollen lens fibers with abnormally retained nuclei are sometimes referred to as bladder or balloon cells (arrows). *Image courtesy of the U.S. National Toxicology Program.*

Age-related cataract formation is well recognized in the rat, most commonly nuclear or posterior cortical, although posterior subcapsular and anterior cortical cataracts are also seen. In the Sprague–Dawley rat, lesions of the posterior lens cortex and capsule are most frequent and plaque opacities attached to the posterior surface of the lens are quite common in old animals, with 8–14% of males and 3–8% of females showing this feature at 100–110 weeks. The effect is thought to be a result of photooxidation, and caloric restriction (which has antioxidant effects) has been shown to significantly delay cataract formation in pigmented rodents, but not in albino animals, which lack any light protection related to pigment. Cortical cataracts are promoted by the same factors

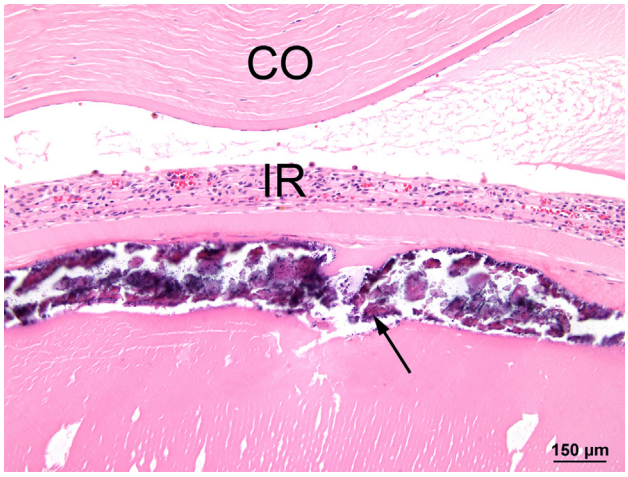


**FIGURE 16.20** Prominent anterior subcapsular mineralization (arrow) in a cataract. *Image courtesy of the U.S. National Toxicology Program.*

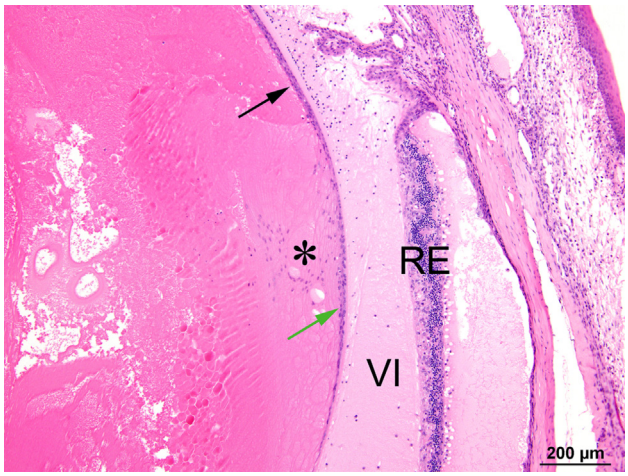


**FIGURE 16.21** Cataractous lens exhibits hyperplasia (black arrow) and posterior migration of anterior epithelial cells (green arrow) beyond their normal limit at the lens bow (*). The retina exhibits atrophy/degeneration and detachment, and the vitreous contains proteinaceous fluid and inflammatory cells. *Image courtesy of the U.S. National Toxicology Program.*

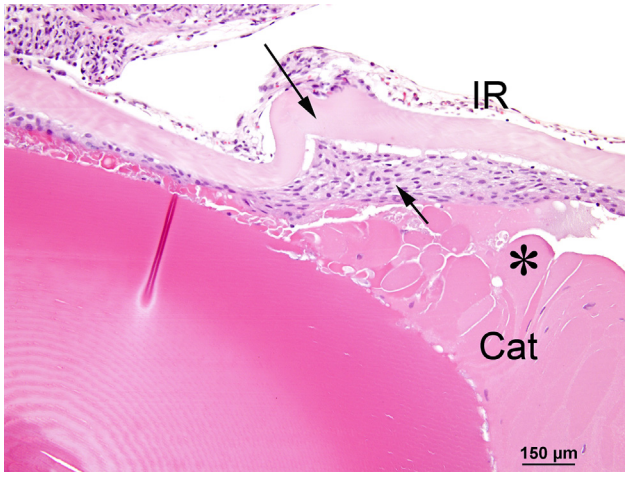


**FIGURE 16.22** Cataractous lens exhibits thickening and wrinkling of the anterior lens capsule (long arrow) and subcapsular hyperplasia of the anterior lens epithelium (short arrow). Note the swollen, condensed, or irregular lens fibers (*) in the cataract. *Image courtesy of the U.S. National Toxicology Program.*

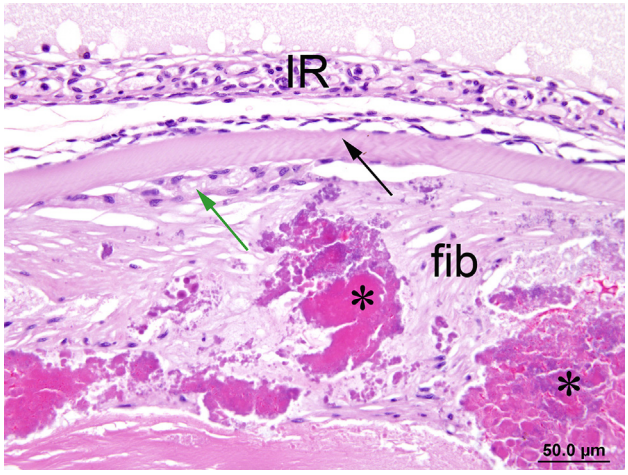


**FIGURE 16.23** Anterior cataract exhibits subcapsular fibrosis (fib) surrounding coarse masses of fragmented, condensed lens fiber material (*). There is hyperplasia (green arrow) of the lens epithelium underlying the anterior capsule (black arrow). *Image courtesy of the U.S. National Toxicology Program.*

described next for retinal degeneration. UV light is absorbed by the lens epithelium and the lens fibers, and has been incriminated in the production of cortical cataracts in mice and in humans. Long–Evans rats administered the photoactive agent 8-methoxypsoralen—which binds to lens epithelium—and subsequently exposed to UV radiation may exhibit hyperplasia of the epithelial cells, resulting in cataract formation.

### 4.1.4. Retinal Degeneration and Atrophy

The outer nuclear layer of the young adult rat retina is approximately 12 nuclei thick in the central area, thinning to six to eight nuclei in the peripheral retina. The distribution and pattern of degenerative lesions may aid in identifying the likely cause. Retinal degeneration can occur spontaneously, as a result of excessive exposure to light, with advancing age, or secondarily to increased intraocular pressure. With any of the former three, the lesion is characterized by the progressive loss of photoreceptors, with associated thinning—and eventual loss—of the overlying nuclear layers. In contrast, elevated intraocular pressure results in a form of retinal degeneration which starts at the ganglion cell and inner nuclear layers, progressing from the inside out.

Displaced photoreceptor cell nuclei (photoreceptor nuclei external to the outer limiting membrane, within the photoreceptor layer or subretinal space) have been observed in the normal rat retina. These peripherally displaced nuclei occur most commonly in young, developing, and aged retinas at the periphery and around the posterior pole. Displaced nuclei generally have a normal density of chromatin, however, pyknotic nuclei are occasionally observed. The biological significance of this phenomenon is not completely clear; however, it is believed to be a factor in the gradual loss of photoreceptor cells in the normal retina. Displaced photoreceptors have been observed in a variety of species in addition to rats, including humans, monkeys, pigs, cats, dogs, rabbits, guinea pigs, mice, hamsters, whales, and dolphins.

#### 4.1.4.1. Spontaneous Retinopathies

The Royal College of Surgeons rat suffers an inherited retinal dystrophy and has become a widely used model for retinal rescue using biosimilars or cell-based therapies. A genetic mutation in the cells of the RPE prevents the normal phagocytosis of the outer segment disks of the photoreceptors and initiates apoptosis of photoreceptors in these animals by 25 days of age. This programmed cell death is restricted to, and results in rapid loss of, the photoreceptors, with the cellularity of the outer nuclear layer in the posterior pole being reduced by 70% at 60 days of age. A spontaneous unilateral degeneration of the retina and optic nerve has been observed in F344 rats less than 1 year of age with no other ocular lesions.

Chorioretinal atrophy, or focal linear retinopathy, has been described in 1−5% of Sprague−Dawley rats and has been recognized occasionally in Wistar rats. These lesions are recognized on indirect ophthalmoscopic examination as irregular areas of hyper-reflectivity with prominent large choroidal blood vessels and a decrease in smaller caliber vessels. Histologically, the lesion is characterized by areas of retinal degeneration with loss of photoreceptors and nuclei and increased cellularity of the underlying choroid. The initial lesion appears to be in the RPE, although this is transient and rarely identified; some affected animals have a history of previous anterior uveitis. Although this lesion is likely to have some genetic basis, the heritability is poorly predictable. Spontaneous retinal degeneration has also been reported in the Wistar-derived WNIN/Ob obesity model.

#### 4.1.4.2. Exposure to Light

Before the introduction of routine cage rotation on long-term toxicology and carcinogenicity studies, both retinal degeneration and cataracts were seen with a higher incidence and severity in albino rats housed in cages closest to the light source. The location of light-induced retinal damage tends to mirror the light path, with more severe damage being seen in the posterior pole than in the peripheral retina. Rats exposed to a 12 h light:dark cycle at 32 footcandles show thinning of the outer nuclear layer of the central superior retina (midway between the ora ciliaris retinae and the optic nerve). From the normal 12 layers at 6 months of age, the cellularity shows progressive reduction to 10, 8, or 6 nuclei or less by 9, 18, and 24 months, respectively. More intense exposure to light—related to increased time of the light cycle or increased intensity of light—or elevated body temperatures may lead to almost complete loss of the photoreceptor and outer nuclear layers. Retinal capillary diameter increases and there is thickening of the basement membrane. With time, the inner nuclear layer will also disappear and capillaries may invade the vitreous and the lens. Albino rats are more susceptible than pigmented strains because melanin in the RPE and uveal tract limits light fluxes in the retina; however, pupillary dilatation can override the protective effect of melanin. Interpretation of toxicity studies may be confounded if photoreceptor loss due to light exposure is exacerbated by test articles that cause mydriasis (Figures 16.24 and 16.25).

Rats examined by indirect ophthalmoscopy 3 days after light exposure on phototoxicity studies are frequently noted to have a focal retinal lesion in the inferior retina—related to the focal concentration of the light at this region in the anesthetized and restrained animal. These photic lesions are also characterized by loss of photoreceptors and decreased cellularity of the outer nuclear layer, together with a scant cellular infiltrate. The lesion is seen in untreated control animals and should not be confused with an induced phototoxic lesion.

#### 4.1.4.3. Age-Related Retinal Degeneration

Age-related retinal degeneration is common in rats and may be related to senescent changes as well as environmental factors. Selective and progressive loss of photoreceptors and a decrease in the cell density of all three nuclear layers occurs in the retina of aged rats even when they are exposed to very low intensities of fluorescent light. The change involves the entire retina, although it may be more readily detected in the peripheral retina. This change parallels declines in retinal glucose utilization, taurine content, protein solubility, and levels of GSH and ascorbate (AsA). Staining for glial fibrillary acidic protein has indicated that Müller cell changes precede the photoreceptor degeneration in this condition. Caloric restriction has been shown to attenuate oxidative stress and sustain the pool of protective factors, such as GSH and AsA, retarding this degeneration in the neural retina of the pigmented Brown Norway (BN) rat, but not in the albino rat (Figures 16.26 and 16.27).

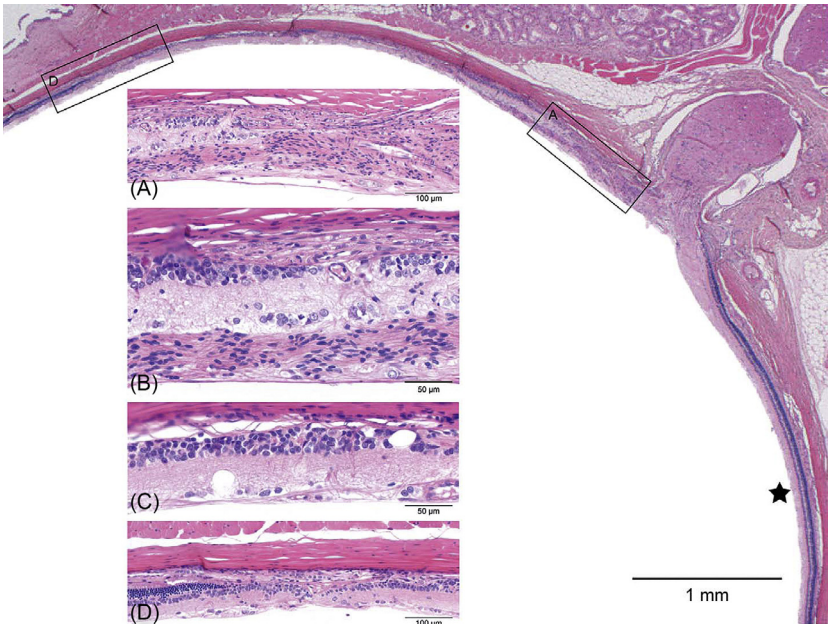


**FIGURE 16.24** Light-induced retinal degeneration in an albino rat from a 2-year carcinogenicity study. There is a distinct difference in thickness of the retina on either side of the optic disk. The ★ marks the relatively normal inferior retina. Approximately 50% of the superior retina is markedly reduced in thickness and shows different degrees of retinal atrophy. These begin adjacent to the disk (boxed area-.A, Figure 16.24A) and extend to the midperiphery (boxed area-D, Figure 16.24D); intervening regions are illustrated in 16.24B and C. (A) The retina nearest the optic disk shows full-thickness loss of retinal layer organization and fibrous connective tissue in the vitreal aspect of degenerating retina. (B) The same tissue overlays the ganglion cell layer; the inner nuclear layer is moderately reduced and abuts the choroid and sclera. The outer retinal layers and RPE are absent. (C) Microcystoid vacuoles are present within remnant inner retinal layers. (D) There is an abrupt transition into less affected retina with preservation of RPE, outer nuclear, and photoreceptor layers. *de Vera Mudry et al. (2013); reprinted by permission of Sage Publications.*

#### 4.1.4.4. Retinal Degeneration Secondary to Increased Intraocular Pressure

Increased intraocular pressure (glaucoma) results in a particular form of ischemia characterized by the release of glutamate into the vitreous. This initiates the death of ganglion cells, and some amacrine cells, which contain ionotropic glutamate receptors. The resulting retinal atrophy affects the ganglion cells and inner nuclear layer prior to visible effects on the outer nuclear layer and photoreceptors: the lesion progresses from the inside out rather than the other forms of retinal atrophy, which progress from the outside in.

### *4.1.5. Microcystoid Degeneration of the Retina*

Microcystoids are small vacuoles, devoid of content, and are occasionally seen in conjunction with age-related retinal degeneration in the peripheral retina of rats. Typically, they are located in the outer regions of the inner plexiform layer. Such lesions may occasionally coalesce, forming larger cystoids with, or without, cellular projections into the cystoid lumen. Microcystoids have been seen in the inner plexiform layer and inner nuclear layers throughout the retina of dystrophic Royal College of Surgeons rats from 3 months of age. Microcystoids may also be observed in association with light-induced retinal degeneration or retinal detachment.

### *4.1.6. Pigment Accumulation*

Lipofuscin pigment accumulates in the RPE with aging, but is not easily recognized in routine sections; specific diagnosis is not recommended without the use of special stains. Cytoplasmic lipofuscin granules increase by 70% between 28 and 117 weeks of age. The RPE plays a role in vitamin A uptake, and high vitamin A levels or vitamin E deficiency result in lipofuscin deposition in the cytoplasm of the RPE.

### *4.1.7. Vacuolar Degeneration of the Choroid*

Small vacuoles are infrequently observed in the choroid of aging rats. The vacuoles may cause the choroid to be slightly thickened, but the overlying retina appears normal. The vacuoles may be due to an expansion of the intercapillary space in the choroid, and their significance is unknown.

## 4.2. Adnexa

In rats, lacrimal gland acini change gradually with age from serous to seromucous to mucous acini. The acinar cell type in young rats is predominantly serous. This is

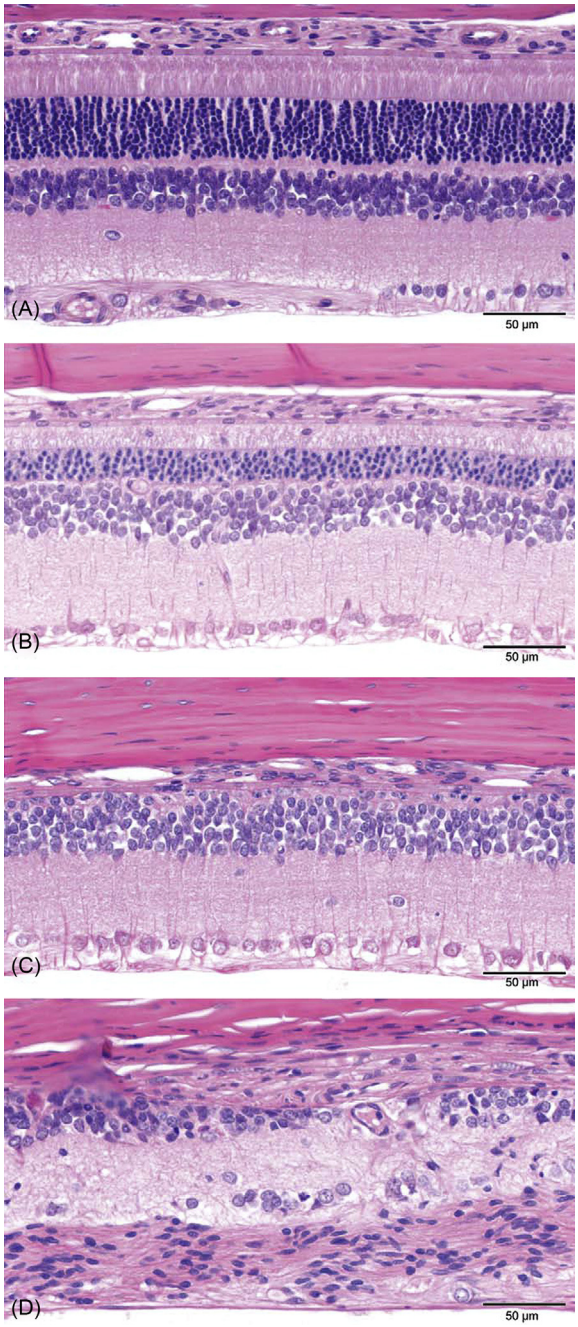


**FIGURE 16.25** Example of a generally accepted grading scale (normal→minimal→slight→moderate→severe) to evaluate retinal atrophy in rat toxicity studies. (A) Normal retina: the different retinal layers are distinct, photoreceptor inner and outer segments are elongated, and outer nuclear layer is intact. (B) Slight retinal atrophy: different layers remain distinct, but the outer nuclear layer is reduced in thickness, and macrophages are present in the photoreceptor layer. (C) Moderate retinal atrophy: the RPE, photoreceptors, and most of the outer nuclear layer are lost; the outer plexiform layer is not present. The inner nuclear layer remains relatively intact albeit irregular. (D) Severe retinal atrophy: there is marked disruption of the normal retinal architecture with loss of retinal layer organization. Remnants of inner nuclear and ganglion cells remain. *de Vera Mudry et al. (2013); reprinted by permission of Sage Publications.*

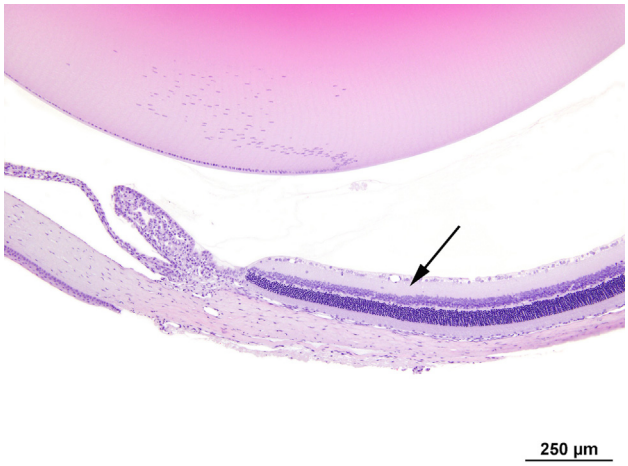


**FIGURE 16.26** Normal peripheral retina (arrow).

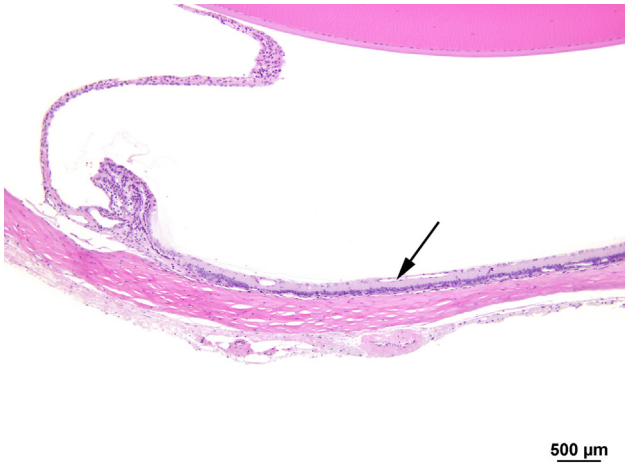


**FIGURE 16.27** Retina with peripheral atrophy (arrow); note the marked thinning due to hypocellularity or the absence of retinal layers (compare to a normal retina shown in Figure 16.26).

also true of 9-month glands, although there is a significant decrease in the overall distribution of the serous acini when compared to the younger glands. In consequence, there are increases in both seromucous and mucous acini. By 12 months, there is a significant increase in the relative occurrence of seromucous acini at the expense of serous acini. Degeneration of the Harderian gland and extraocular muscles is a consequence of continuous fluorescent illumination.

## 5. INFLAMMATORY AND VASCULAR LESIONS

### 5.1. Eye

Keratitis (inflammation of the cornea) occurs occasionally and may be secondary to trauma, desiccation, bacterial

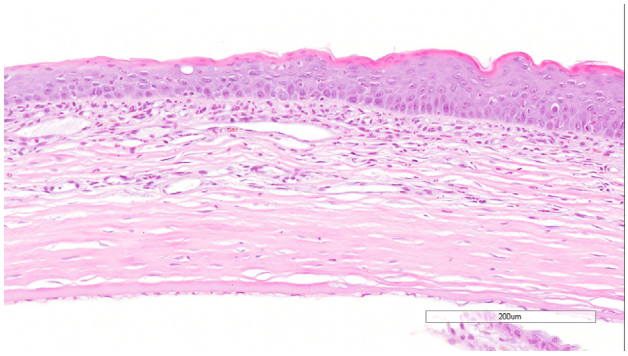

FIGURE 16.28 Hyperplasia of the corneal epithelium. Note inflammatory cell infiltrates and vascularization of the stroma (arrows).

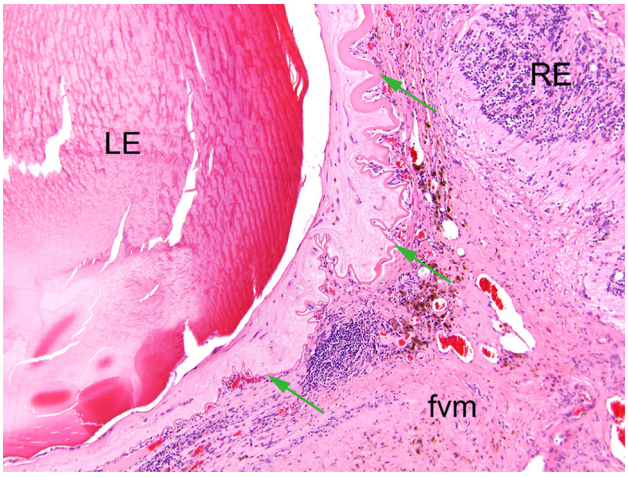


FIGURE 16.29 A fibrovascular membrane (fvm) fills the vitreous and adheres to the cataractous lens (LE) and the detached, degenerate retina (RE). Green arrows indicate the markedly wrinkled and focally thickened posterior lens capsule. *Image courtesy of the U.S. National Toxicology Program.*

infections, or sialodacryoadenitis virus (SDAV) infection, which decreases lacrimal secretions. The acute lesion is characterized by an infiltrate of neutrophils in the epithelium and stroma, and the anterior chamber may contain inflammatory cells and fibrin. There may be focal to diffuse hyperplasia of the corneal epithelium with occasional nests of hyperplastic epithelial cells in the stroma. Severe keratitis is associated with hemorrhage, necrosis, ulceration, vascularization, fibrosis, and conjunctivitis. There is some evidence that mycoplasmas are associated with, and may cause, conjunctivitis (Figure 16.28).

Uveitis is rarely seen as a spontaneous lesion, but can be induced experimentally as an autoimmune uveoretinitis by injection of certain ocular antigens. It is characterized by a focal to diffuse infiltrate of neutrophils and lymphocytes in the retina and choroid. Retinitis is rare as a primary lesion, but the retina can be involved secondarily with other inflammatory processes of the eye. Congenital retinitis occurs by maternal exposure to the lymphocytic choriomeningitis virus. The pups exhibit varying degrees of inflammation with retinal degeneration (loss of photoreceptor cells) and, in severe cases, retinal detachment.

Panophthalmitis is characterized by inflammation involving the entire eye. In some cases, it may be associated with, or secondary to, ocular damage related to high light intensity. There may be chronic uveitis, keratitis, and cataract formation; severe lesions may result in phthisis bulbi (shrunken, fibrotic globe).

Fibrovascularization or organization of the vitreous body is seen in rats with advanced retinal degeneration. Initially, a delicate fibrovascular network is formed in the vitreous body accompanied by hemorrhage, pigment-laden macrophages, and other inflammatory cells. Newly formed capillaries can be seen extending into the vitreous body. Progression leads to mineralization and even cartilaginous metaplasia (Figure 16.29).

Hemorrhage with accumulation of blood between the outer nuclear layer and pigment epithelium of the retina is sometimes observed. The hematoma may reach nearly half the size of the retinal hemisphere, with the retinal tissue over the hematoma completely separated from the pigment epithelium. The cause is unknown. Hemorrhage in the anterior segment or vitreous is often associated with persistent fetal vasculature.

## 5.2. Adnexa

Viral infections (rat coronavirus and SDAV) are the most common cause of clinically significant inflammatory processes in the lacrimal and Harderian glands. Rats acutely infected with SDAV show swelling of the glands, epiphora with red staining of periocular and perinasal fur (chromodacryorrhea), and transient blepharospasm. Histologically, there is degeneration and necrosis of secretory cells with edema and infiltration by neutrophils and macrophages. Chronic lesions are characterized by lymphocytic infiltrates and squamous metaplasia (Figure 16.30).

In aging rats, pigment accumulation, fibrosis, and inflammatory infiltrates are sometimes found in the Harderian gland. Likewise, changes that occur with age in Sprague–Dawley lacrimal glands include increased periductal fibrosis, acinar atrophy, and inflammatory cell infiltrates, which include lymphocytes and mast cells. Meibomian glands are frequently infiltrated with a small number of lymphocytes or neutrophils (Figure 16.31).

# 6. HYPERPLASTIC AND NEOPLASTIC LESIONS

Epithelial and mesenchymal neoplasms arising from the skin of the eyelids may be seen and are generally similar

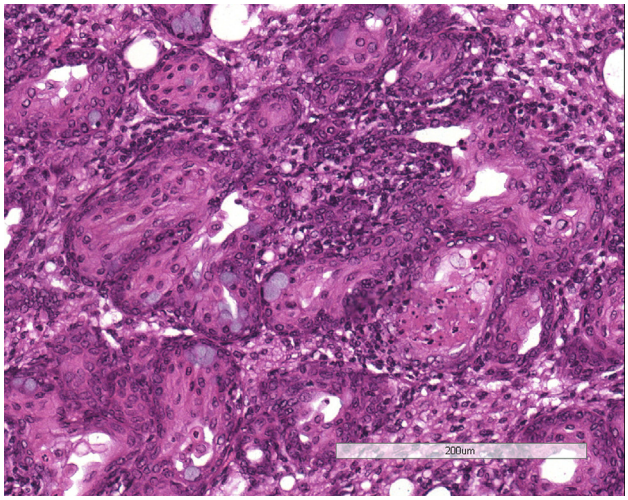


**FIGURE 16.30** Squamous metaplasia of Harderian gland following SDAV infection.

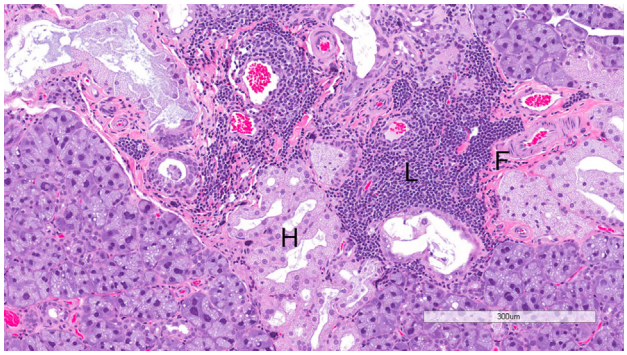


**FIGURE 16.31** Exorbital lacrimal gland of aging Wistar rat showing fibrosis (F), multifocal lymphocytic infiltrates (L), and Harderian gland alteration (H).

to those occurring in the skin at other locations. These are described in Chapter 17 and are not discussed further here. Rarely, malignant neoplasms of neural crest origin with similarities to melanoma and melanotic schwannoma occur in the eyelids as well as the pinna. This neoplasm is described in Chapter 15.

Spontaneous neoplasms of the lacrimal or Harderian glands are rare, although adenomas of the Harderian gland may be successfully induced. Spontaneous intraocular neoplasms in the rat are rare, but are seen most frequently in the uveal tract (iris, ciliary body, and choroid). Neoplasms can be induced by intraocular injection of carcinogens.

## 6.1. Eye

### 6.1.1. Dermoid

Dermoid is a rare lesion in the rat. This congenital lesion appears grossly as an elevated white plaque with numerous fine hairs, arising from the normally hairless cornea or conjunctiva. Histologically, it consists of a fibrous connective tissue stroma, containing hair follicles and sebaceous glands, covered by a stratified squamous epithelium.

### 6.1.2. Squamous Cell Papilloma and Carcinoma

Squamous cell neoplasms have been seen on the cornea, conjunctiva, and eyelids of rats. Their histological features are similar to those occurring on the skin and elsewhere. Squamous cell papilloma is distinguished from carcinoma by its absence of invasion of the stroma by the atypical squamous cells; growth is typically exophytic, but may be endophytic in the case of inverted mucoepidermoid papilloma. The carcinomas show breach of the basement membranes by invasive, atypical epithelial cells and may exhibit a papillary growth pattern in addition to downward growth into the corneal stroma. Dyskeratosis and epithelial pearl formation are often observed, and the corneal stroma may be markedly thickened by fibrosis and the infiltration of mixed inflammatory cells.

### 6.1.3. Melanocytic Hyperplasia

Nonneoplastic melanocytic hyperplasia has been reported in the uveal tract of the BN rat and in the eyelid of a BN x F344 cross. There is minimal displacement of normal structures and the lesions are characterized by small aggregates of pigmented, polygonal melanocytes with minimal atypia.

### 6.1.4. Melanoma, Uveal, Malignant

Spontaneous uveal melanoma in the rat most frequently arises in the region of the ciliary body and is typically unilateral; such spontaneous tumors have been recorded in F344, Wistar, and Sprague–Dawley rats with involvement of the iris, ciliary body, or choroid. Chemically induced melanomas may arise from any site in the uveal tract and have been induced by intravitreal instillation (nickel subsulfide in the F344 rat and nickel sulfide in the August Copenhagen Irish rat), oral administration (ethionine and *N*-2-fluorenylacetamide in the Wistar rat), and subcutaneous administration (urethane and *N*-hydroxyurethane in the August rat). In albino strains, these tumors are amelanotic.

Melanomas are usually composed of spindle cells arranged in parallel bundles and form whorls, sometimes with a perivascular orientation. The spindle cells have poorly defined cell boundaries, scant to moderate cytoplasm, fusiform nuclei, and indistinct nucleoli. Other tumors may include areas incorporating poorly defined epithelioid cells loosely scattered among the spindle-shaped cells. Such epithelioid cells have pale-staining cytoplasm, poorly defined cell borders, and large, ovoid nuclei with or without nucleoli; rarely, enlarged

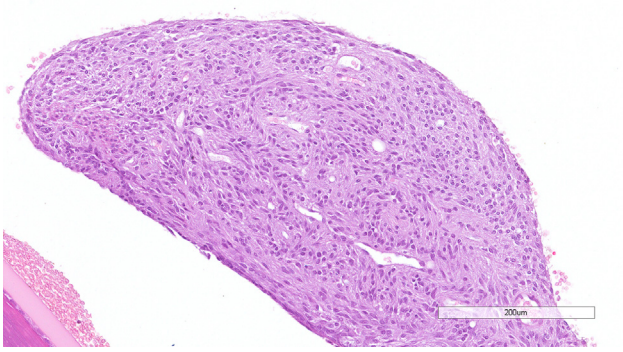

FIGURE 16.32 Amelanotic melanoma of the iris in a Wistar rat.

epithelioid cells having large, bizarre nuclei with prominent nucleoli may be seen. Mitotic figures are common and areas of necrosis may be present. The cells may contain argyrophylic filaments and scant yellow-brown pigment. The neoplastic cells are often positive when stained with immunohistochemical markers for the S100 protein and vimentin intermediate filaments. Ultrastructurally, the neoplastic cells contain intracytoplasmic microtubules including filamentous or membranous structures. Such immunohistochemical staining and electron microscopy are usually necessary to distinguish the amelanotic tumors from schwannoma or leiomyoma. Chemically induced melanomas have been shown to contain premelanosomes and melanosomes that may stain positively with the Fontana reaction for melanin (Figure 16.32).

### 6.1.5. Leiomyoma, Uveal

Iridal leiomyoma has been reported in the Wistar and Sprague–Dawley rat. The tumors are composed of spindle-shaped cells having granular eosinophilic cytoplasm with poorly defined borders and elongated nuclei with rounded ends (cigar-shaped) and stippled chromatin. These cells are arranged in closely packed interlaced bundles and whorls that may form palisades around blood vessels in a well-vascularized stroma. The cells may stain positive with markers for desmin, Staining for S100 protein is negative.

### 6.1.6. Leiomyosarcoma and Hemangiosarcoma

Leiomyosarcoma and hemangiosarcoma have been reported to occur rarely in the eye of the rat.

### 6.1.7. Schwannoma, Intraocular, Malignant

Schwannomas of the uveal tract have been reported in Wistar and F344 rats. These tumors are composed of plump, spindle-shaped cells having abundant eosinophilic vacuolated cytoplasm and normochromic, ovoid to short elongate nuclei that may include a small eosinophilic nucleolus. The cells are arranged in a fascicular perivascular pattern, with occasional formation of pseudorosettes. Areas of necrosis and mitotic figures may be seen. The cells stain positive for S100 protein.

### 6.1.8. Retinoblastoma

Spontaneous retinoblastoma has not been reported in the rat, but such tumors have been induced by nickel compounds, human adenovirus type 12, and 5-iododeoxyuridine. The neoplasms are characterized by proliferation of small, uniform, undifferentiated cells that have hyperchromatic nuclei with an irregular, round or slightly elongate profile, and scant cytoplasm with indistinct cell borders. Neuroepithelial rosettes or perivascular pseudorosettes are sometimes seen. Mitoses are frequent and hemorrhage and areas of necrosis may be present. Ultrastructurally, characteristic triple-membrane structures involving the nuclear envelope and cell attachments by zonula adherens and macular occludens may be present.

## 6.2. Harderian Gland

### 6.2.1. Hyperplasia, Acinar

Hyperplasia of the Harderian gland may occur as a regenerative response to degeneration and inflammation or as a primary proliferative lesion. Hyperplasia without evidence of degeneration is uncommon. Alveolar architecture is retained; however, there is an increase in alveolar cells, which may cause the epithelium to appear pseudostratified or folded. If the hyperplasia is severe, the alveolar walls may develop small papillary projections distorting the regular arrangement of the alveoli. Generally, there is no compression of the adjacent parenchyma. The hyperplastic alveolar cells are usually enlarged with variable staining characteristics. Nuclear size and shape are unaffected and mitotic figures are rare.

### 6.2.2. Adenoma

Harderian gland neoplasms are rare in the rat. Spontaneous adenomas have been reported. Neoplasia of the Harderian gland has been induced in the Medical Research Council rat by the repeated injection of urethane, and in rats maintained on a low-fat diet containing 2-acetylamino-fluororene. Adenomas are characterized by expansile growth and compression of the adjacent tissue, but these tumors are not usually encapsulated. They are composed of enlarged cells, which may be pale staining. Nuclei may also be large, but remain uniform, and mitotic activity is rare. The tumors may have a papillary growth pattern and the alveolar epithelium may appear pseudostratified or stratified.

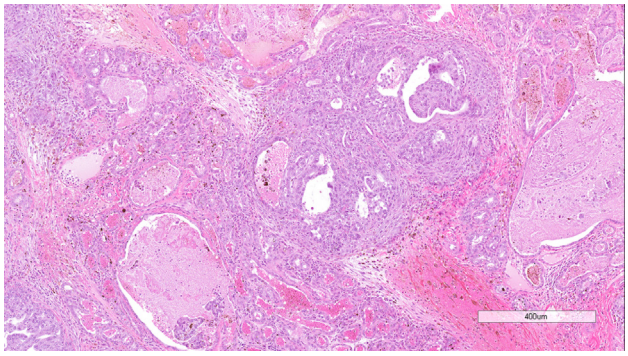

FIGURE 16.33 Harderian gland adenocarcinoma in a Wistar rat showing tubular and solid growth patterns, infiltrative growth, and scirrhous reaction.

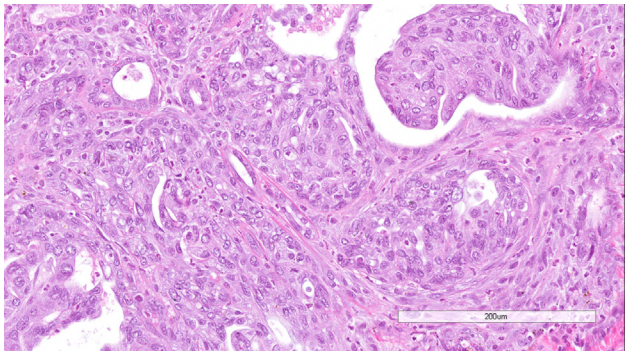

FIGURE 16.34 Higher magnification of Figure 16.33.

### 6.2.3. Adenocarcinoma

Adenocarcinomas have been reported in the Harderian gland of rats. An expansive, enlarging lesion that distorts the surrounding tissue, adenocarcinoma is distinguished from adenoma by loss of the normal lobular pattern, increased cellular pleomorphism and atypia, and evidence of local invasion. The development of a scirrhous reaction is also indicative of malignancy. Better-differentiated adenocarcinomas consist of cuboidal to columnar epithelial cells arranged in tubular or gland-like structures. Less well-differentiated or anaplastic neoplasms exhibit stratification of the epithelium or solid sheets of cells. Foci of necrosis and fibrosis may be present (Figures 16.33 and 16.34).

## 6.3. Lacrimal Gland

### 6.3.1. Hyperplasia, Acinar

Hyperplasia of the lacrimal glands is usually secondary to degenerative or inflammatory lesions (i.e., regenerative hyperplasia associated with SDAV infection). Primary spontaneous or chemically induced hyperplasia of the lacrimal gland has not been reported in the rat.

### 6.3.2. Adenoma

Adenomas of the lacrimal gland have been reported in rats. They are expansile lesions that compress or displace the normal parenchyma. The normal lobular and acinar arrangement within the mass is distorted and/or irregular, but the acinar cells are well-differentiated and uniform cuboidal cells forming tubular and acinar structures. Intercalated ducts are not usually observed. Mitoses are infrequent.

### 6.3.3. Adenocarcinoma

Adenocarcinoma has also been reported in the rat and is distinguished from adenoma by loss of the normal lobular pattern, increased cellular pleomorphism and atypia, and evidence of local invasion. Acinar cells are moderately well to poorly differentiated, and contain secretory (serous) vacuoles. Cellular pleomorphism and atypia are variable.

### 6.3.4. Hemangioma

Hemangioma has been reported to occur rarely in the rat lacrimal gland.

### 6.3.5. Squamous Cell Hyperplasia, Papilloma, and Carcinoma of the Lacrimal Duct

Squamous cell hyperplasia is frequently observed in the lacrimal duct, often associated with inflammation. Spontaneous squamous cell papillomas or carcinomas of the lacrimal duct are rare, but have been observed in the nasolacrimal duct of rats exposed to vapors of certain carcinogens. These neoplasms are similar to those occurring at other sites.

## 6.4. Optic Nerve

Spontaneous neoplasms of the optic nerve are rare in rats. Meningiomas, schwannomas, ganglioneuromas, and gliomas may involve the optic nerve. Gliomas of the optic nerve are also induced by injection of nickel compounds.

### 6.4.1. Meningioma

Meningiomas (described in detail in Chapter 11) affecting the optic nerve may consist of pleomorphic spindle cells arranged in a whorling pattern, often with a perivascular orientation, or consist predominantly of epithelioid cells forming small concentric whorls that resemble Hassall's corpuscles of the thymus. The neoplasms may demonstrate a positive reaction for the S100 protein. Ultrastructurally, the neoplastic cells have interdigitating cellular processes and numerous desmosomes.

#### 6.4.2. Malignant Schwannoma

Malignant schwannomas of the orbit may arise in the peripheral nerves, as well as the optic nerve. Their morphology is similar to those arising from other cranial or spinal nerves (see Chapter 12).

#### 6.4.3. Ganglioneuroma

Ganglioneuroma of the optic nerve has been reported in the Copenhagen rat.

#### 6.4.4. Glioma

Spontaneous glioma of the optic nerve has been reported in the Sprague–Dawley rat. Glial neoplasms are also induced in the F344 rat by nickel compounds. The induced neoplasms resemble astrocytomas.

## 7. MISCELLANEOUS LESIONS

### 7.1. Eye

#### 7.1.1. Epithelial (Inclusion) Cyst

Epithelial cysts occur rarely in the stroma of the rat cornea and are usually unilateral. These may be congenital or the result of trauma. The cyst wall consists of a keratinized, stratified squamous epithelium several layers thick.

#### 7.1.2. Synechia and Other Sequelae of Intraocular Inflammation

Synechia is usually a sequel to keratitis, iridocyclitis (inflammation of the iris and ciliary body), or conjunctivitis. It is infrequently observed in aging rats. Posterior synechia, the adhesion of the posterior surface of the iris to the lens capsule, is often associated with cataracts. Anterior synechia, the adhesion of the anterior surface of iris to the endothelium of the cornea, usually occurs as a result of severe keratitis. Synechia may be accompanied by variable degrees of hemorrhage and inflammation with exudate or flocculent material in the anterior and posterior chambers. Organization of exudate in the anterior chamber may result in formation of a pre-iridal fibrovascular membrane that often distorts the iris. Organization of exudate in the posterior chamber or anterior vitreous may result in formation of a retrolental fibrovascular (cyclitic) membrane, a circumferential adhesion of the ciliary body to the lens.

#### 7.1.3. Retinal Detachment

Retinal detachment is rarely seen in rats. During tissue processing, artifactual separation of the retina from the pigment epithelium is common. True retinal detachment may be distinguished from an artificial detachment by (1) the presence of fluid in the subretinal space (between the photoreceptors and the pigment epithelium), (2) partial or complete loss of the photoreceptor layer, and/or (3) hypertrophy of the pigment epithelium. The subretinal space usually contains proteinaceous material with a small number of hemosiderin-laden macrophages and cellular debris. The underlying pigment epithelium is usually a single layer of cuboidal cells with small to large cytoplasmic vacuoles. The overlying retina may show microcystoid and/or outer retinal degeneration. Reattachment of the retina may result in atrophy, folding of the retina, and rosette formation.

#### 7.1.4. Retinal Gliosis

Gliosis may be induced in the retina of rats by intraocular injection of nickel compounds. Histologically, gliosis is seen in the ganglion cell layer and consists of increased numbers of disorganized glial cells. Nickel injection also induces fibrous metaplasia of the RPE in rats and may induce gliomas. Gliosis is an uncommon change in aging rats.

### 7.2. Adnexa

#### 7.2.1. Chromodacryorrhea

Chromodacryorrhea is a clinical sign characterized by brick-red tears sometimes mistaken for hemorrhage. The tears result from excessive secretion of porphyrin from the Harderian gland, which can be provoked by nonspecific stimuli, such as stress, and by specific agents, such as cholinergic drugs. In the rat Harderian gland, protoporphyrin IX is the predominant form synthesized in the cytoplasm of acinar cells. Porphyrin secretion increases with age and is stimulated by administration of estradiol plus progesterone; it is decreased by constant light or constant darkness. Excessive production of porphyrin may be due to a failure in the regulation of synthesis by mitochondrial enzymes. Histologically, porphyrin is seen as a yellow-brown pigment within the alveolar lumens (Figure 16.10).

#### 7.2.2. Cytomegaly (Karyomegaly) of the Lacrimal Gland

Cytomegaly of acinar cells with karyomegaly is often seen in the extraorbital, but not the intraorbital, lacrimal gland of rats; it is generally less frequent in females than males. The cytomegalic cells are multifocal in distribution and the affected nuclei are up to three times normal size. The change may be spontaneous (it occurs in rats free of known murine viruses) or induced by murine cytomegalovirus infection (Figure 16.11).

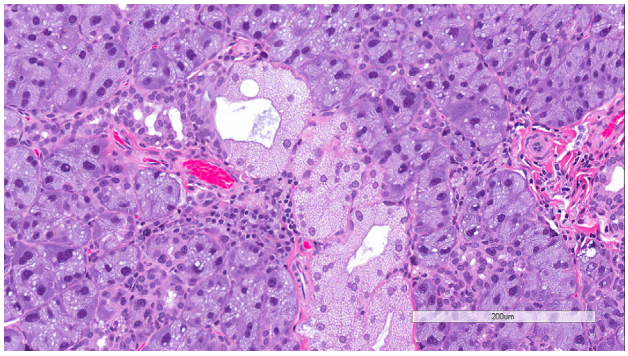

FIGURE 16.35 Exorbital lacrimal gland from a Wistar rat showing Harderian gland alteration.

### 7.2.3. Intranuclear Inclusions of Lacrimal Glands

Intranuclear pseudoinclusions are observed in the acinar cells of the lacrimal glands. The inclusions have been shown to be invaginations of the cytoplasm into the nucleus. These are seen at puberty in males and with testosterone treatment, but are prevented by castration.

### 7.2.4. Harderian Gland Alteration in the Lacrimal Gland

Alveoli with the histological characteristic of the Harderian gland are sometimes found in the extraorbital lacrimal gland. This change may occur in both sexes at 3 months of age, but persists and increases only in males. Estrogens are thought to mediate regression of Harderian gland-like foci in females. The affected alveoli are composed of cuboidal to columnar cells with finely vacuolated cytoplasm and the alveolar lumens are distinct. Grossly, the lesions are recognized as small pale foci (Figure 16.35).

### 7.2.5. Epithelial Cyst of the Nasolacrimal Duct

Epithelial cysts usually associated with inflammation are occasionally found in the submucosa of the nasolacrimal duct. The cysts are usually seen in the portion of the duct lateral to the roots of the upper incisor teeth. The cysts are lined by stratified squamous epithelium and often contain keratin and cellular debris.

## 8. TOXICOLOGIC LESIONS

The eye contains several unique structures including the transparent avascular cornea and lens, the complex metabolically active retina, and the ciliary body, which produces the aqueous humor. Therefore, the toxic lesions encountered in the eye are diverse. There are species and strain differences in sensitivity to the toxicity of various chemicals, and the monkey, dog, and rabbit are more commonly used for studying ocular toxicity than the rat. Various teratogens affect the eye and maternal zinc deficiency results in a high frequency of fetal eye malformations.

Neoplasms of the eye are rarely induced by systemic administration of chemicals, but are observed following the intraocular injection of various compounds. Although Harderian gland neoplasms in mice are relatively frequently induced by chemical exposures and radiation, this is not true in the rat.

## 8.1. Eye

### 8.1.1. Cornea

Tricyclic antidepressant drugs cause small opacities of the cornea of young F344 rats, but not Wistar, Sprague–Dawley, Long–Evans, or Buffalo rats. Histologically, these are punctate lesions on the posterior surface of the cornea consisting of focal eruptions of the corneal endothelium that contain necrotic cells, fibroblasts, collagen, and mineral. Susceptibility to the induction of this lesion decreases with age; adult F344 rats are insensitive. Thallium causes keratitis in rats and dogs, but not in other species including humans. In F344 rats, keratitis is also induced by dimethylamine.

Calcific keratopathy is induced in F344 rats by propylene glycol monopropyl ether (PGPE). The keratopathy is characterized by necrosis and splitting of the corneal epithelium, stromal fibrosis, mineralization, and vascularization. The F344 rat is more sensitive to PGPE than the Sprague–Dawley rat, Hartley guinea pig, or New Zealand white rabbit. The PGPE keratopathy is similar to that induced by morphine sulfate (MS) in the Sprague–Dawley rat. Mineral deposits resulting from PGPE and MS exposure are irreversible, in contrast to those produced by local application of alloxan and/or dihydrotachysterol; the latter disappear from the heavily vascularized corneal stroma after several weeks.

Corneal edema in the rat may be epithelial, stromal, or endothelial. Rats on a protein-deficient diet may have corneal edema affecting all three layers. There is prominent vacuolation of basal cells of the epithelium and separation of the basal plasma membrane from the basement membrane. Endothelial edema is induced in rats by exposure to carbon monoxide, but is transitory and completely resolves within a 24 h period. Histologically, the edema is characterized by swelling and desquamation of the endothelium with thickening of the posterior limiting membrane. The venous sinuses of the iris and ciliary body are congested.

Lipid keratopathy (corneal lipidosis) is induced in rats by amphophilic cationic drugs as part of generalized lipidosis. The human cornea is more severely affected than that of the rat and different rat strains vary in susceptibility. Histologically, the stromal cells appear beaded due to intensely staining cytoplasmic inclusions (phospholipids).

Similar inclusions occur in the endothelial and epithelial (basal cell) layers. Ultrastructurally, lamellated inclusions are found in the cytoplasm of the basal cells, whereas stromal and endothelial cells contain both lamellated and crystalline inclusions.

### 8.1.2. Uvea

Cyclitis is produced in the rat by cyclophosphamide. The ciliary body and processes are distended by eosinophilic fluid containing fibrin and inflammatory cells. The overlying epithelium may show degenerative changes. Melanoma is induced in the iris, ciliary body, and choroid in rats by intraocular injection of nickel subsulfide. Intraocular injection of (*N*-hydroxy-)urethane and *N*-methyl-*N*-nitrosourea has induced melanoma in the eyes of other albino and hooded rats.

### 8.1.3. Lens

In the rat and mouse, the lens develops white opacities when animals are given compounds that interfere with blinking, such as narcotics. These opacities are reversible within a few hours.

Cataracts are produced in the rat by various compounds, but the rat appears to be the only animal that develops cataracts after administration of thallium. Chemically induced cataracts often begin near the equator and extend into the anterior or posterior cortex, but may occur anywhere.

Bisulfan causes cataracts in rats, apparently by preventing epithelial cell mitosis. It acts during the G phase of the cell cycle, permitting normal DNA synthesis, but preventing mitosis. Some of these cells undergo degeneration and necrosis. Because the cells in the equatorial zone have the shortest intermitotic time, they are affected first, leading to disorganization of the nuclear bow and lens fibers. Triparanol, a blood-cholesterol-lowering agent that inhibits cholesterol synthesis, also induces cataracts in rats. It causes a 10-fold increase in lens sodium content with hydration and swelling of the lens fibers. Following cessation of treatment, the cataracts are reversed as new fibers are laid down in the periphery, excess $Na^+$ and water are pumped out, and $K^+$ levels are returned to normal. Sodium selenite induces nuclear cataract in 4–6 days if given to suckling rats before completion of the critical lens maturation period at approximately day 16. Sodium selenite appears to alter lens epithelial metabolism, resulting in calcium accumulation, calpain activation, and proteolysis and precipitation of crystallins in the nucleus. Cataracts are also experimentally induced in rats by feeding a diet containing high levels of galactose. Galactose is phosphorylated to galactose-6-phosphate or reduced by aldose reductase to dulcitol. Because dulcitol is not further metabolized, it accumulates in the lens and exerts a strong osmotic force, drawing water into the lens. The excessive hydration of the lens produces the initial vacuolization and opacification. However, continued feeding results in an irreversible mature nuclear cataract.

### 8.1.4. Retina

Mitosis of cells in the retina is not seen in adult rats, but is induced by kainic acid or by experimental occlusion of the central retinal vessels followed by reperfusion. This suggests a causal relationship in proliferative retinopathies of humans, where retinal ischemia and retinal glial and vascular cell proliferation coincide.

The primary target cell in toxic retinopathy is either the photoreceptor cell or the pigment epithelium. In the rat, photoreceptor cell toxicity may be due to a depletion of critical substances required by the cell or a direct effect of the toxic agent. Taurine plays an important role in maintaining photoreceptor cell structure and function. In the rat, more than half of the retinal store of taurine is located in the photoreceptor layer, and depletion causes degeneration of these cells in rats as well as cats. Retinal taurine deficiency induced by vigabatrin, a GABA-transaminase inhibitor used to treat seizures, causes peripheral outer retinal disorganization and widespread cone degeneration in rats. Taurine transport antagonists, such as guanidinoethyl sulfonate, inhibit taurine uptake by the pigment epithelium and produce photoreceptor cell degeneration. Initial histological abnormalities are outer segment vesiculation and disorganization and inner segment swelling with eventual loss of photoreceptors.

Lead exposure during early postnatal development in rats selectively causes rod photoreceptor cell degeneration. Histologically, total retinal thickness decreases 10–20% due to cell loss in the outer and inner nuclear layers. Ultrastructurally, rod outer segments are swollen and disorganized, and there are large accumulations of beta-glycogen particles in mitochondria.

Selective toxicity to the photoreceptor cell is induced in the rat by various compounds, but the pathogenesis largely remains unknown. Amoscanate (4-isothiocyanato-4′-nitrodiphenylamine) and iodoacetate cause selective degeneration of rat photoreceptors. Amoscanate also causes selective damage to circumscribed areas of the brain adjacent to lateral ventricles. Dogs and monkeys do not develop either morphological change. The alkylating agents *N*-methyl- and *N*-ethyl-*N*-nitrosurea also induce photoreceptor necrosis.

Toxic retinopathy may also result from changes in the pigment epithelium. Zinc is the most abundant metal in the rat neuroretina; under ambient light, zinc is localized predominantly to the inner part of the photoreceptor inner segments and in the inner nuclear and plexiform layers. Zinc-deficient diets cause impairment of dark adaptation

and the accumulation of lipofuscin (pigmented rats) or nonlipofuscin, osmiophilic inclusions (albino rats) in the RPE. Administration of transitional trace metal chelators such as dithizone has a similar effect, which leads to disorganization and degeneration of photoreceptor outer segments. In contrast, the presence of zinc potentiates light- or ischemia-induced retinal injury.

Beta secretase inhibitors developed to treat Alzheimer's disease may induce RPE hypertrophy in rats due to cytoplasmic accumulation of autofluorescent material, with (likely secondary) photoreceptor degeneration. Severe RPE hypertrophy may result in retinal detachment. Cationic amphophilic drugs, such as the tricyclic antidepressants, and various aminoglycosides interfere with phospholipid degradation, resulting in the accumulation of crystalloid cytoplasmic inclusions in the RPE and other retinal cells. Inhibition of lysosomal phospholipid degradation by chloroquine induces membranous phospholipid inclusions in ganglion cells and, to a lesser extent, the RPE and photoreceptors. Cytoplasmic expansion and vacuolation of the RPE and Müller cells precede cell death in rats given intravitreal triamcinolone; vacuoles correspond to degenerate mitochondria. Pigment epithelium necrosis has been induced by oral schistosomicidal aminophenoxyalkanes such as 1,4,-bis(4-aminophenoxy)-2-phenylbenzene, high intravenous doses of sodium or potassium iodate, and intravitreal injection of L-ornithine hydrochloride, a model of gyrate atrophy of the retina and choroid in humans. D,L-2-amino-3-phosphonopropionate administration to neonatal rats alters metabotropic glutamate receptors, inducing degeneration and necrosis in multiple outer retinal cell types. Retinoblastoma has been induced in the retina of rats by 5-iododeoxyuridine.

### *8.1.5. Vitreous Body*

Cartilaginous metaplasia is induced in the vitreous of rats by intraocular injection of nickel compounds. The gelatinous substance of the vitreous body is nearly replaced by fibrous tissues and metaplastic cartilage.

### *8.1.6. Optic Nerve*

Glioma and meningioma are induced in the optic nerve of rats by injection of nickel compounds. The histological appearance of the glioma resembles that of astrocytic glioma seen in human neurofibromatosis.

## 8.2. Adnexa

Degeneration and necrosis in the Harderian gland of rats is sometimes caused by injection of local anesthetics or blood sampling from the retrobulbar area. Affected acini and ducts are filled with cellular debris and lined by basophilic epithelial cells, which may represent early stages of regeneration.

## BIBLIOGRAPHY


Ackerman, L.J., Yoshitomi, K., Fix, A.S., Render, J.A., 1998. Proliferative lesions of the eye in rats, OSS. Guides for Toxicologic Pathology. STP/ARP/AFIP, Washington, DC.

Albert, D.M., Gonder, J.R., Papale, J., Craft, J.L., Dohlman, H.G., Reid, M.C., et al., 1982. Induction of ocular neoplasms in Fischer rats by intraocular injection of nickel subsulfide. Invest. Ophthalmol. Visual. Sci. 22, 768–782.

Albert, D.M., Puliafito, C.A., Haluska, F.G., Kimball, G.P., Robinson, N.L., 1986. Induction of ocular neoplasms in Wistar rat by *N*-methyl-*N*-nitrosourea. Exp. Eye Res. 42, 83–86.

Alexander, J.H., Young, J.A., van Lennep, E.W., 1973. The ultrastructure of the duct system in the rat extraorbital lacrimal gland. Z. Zel/forsch. Mikrosk. Anat. 144, 453–466.

Ali, Sowden, 2011. Regenerative medicine: DIY eye. Nature. 472, 42–43.

Apple, D.J., Naumann, G.O.H., 1986. Pathology of the Eye. Springer-Verlag, New York, NY.

Artal, P., De Tejada, P.H., Tedós, C.M., Green, D.G., 1998. Retinal image quality in the rodent eye. Vis. Neurosci. 15, 597–605.

Balazs, T., Ohtake, S., Noble, J.F., 1970. Spontaneous lenticular changes in the rat. Lab. Anim. Care. 20, 215–219.

Baskin, S.I., Cohen, E.M., 1978. Senile cataract model: biochemistry and morphology of the aging lens. Adv. Exp. Med. Biol. 97, 308.

Bassett, E.A., Wallace, V.A., 2012. Cell fate determination in the vertebrate retina. Trends Neurosci. 35, 565–573.

Beaumont, S.L., 2002. Ocular disorders of pet mice and rats. Vet. Clin. Exot. Anim. 5, 311–324.

Bellhorn, R.W., Korte, G.E., Abrutyn, D., 1988. Spontaneous corneal degeneration in the rat. Lab. Anim. Sci. 38, 46–50.

Boros, J., Newitt, P., Wang, Q., McAvoy, J.W., Lovicu, F.J., 2006. *Sef* and *Sprouty* expression in the developing ocular lens: implications for regulating lens cell proliferation and differentiation. Semin. Cell Dev. Biol. 17, 741–752.

Braekevelt, C.R., Hollenberg, M.J., 1970. The development of the retina of the albino rat. Am. J. Anat. 127, 281–302.

Brock, W.J., Somps, C.J., Torti, V., Render, J.A., Jamison, J., Rivera, M.I., 2013. Ocular toxicity assessment from systemically administered xenobiotics: considerations in drug development. Int. J. Tox. 32, 171–188.

Bromberg, B.B., Welch, M.H., 1985. Lacrimal protein secretion: comparison of young and old rats. Exp. Eye Res. 40, 313–320.

Brownscheidle, C.M., Niewenhuis, R.J., 1978. Ultrastructure of the harderian gland in male albino rats. Anat. Rec. 190, 735–754.

Bruner, R.H., Keller, W.F., Stitzel, K.A., Sauers, L.J., Reer, P.J., Long, P.H., et al., 1992. Spontaneous corneal dystrophy and generalized basement membrane changes in Fischer 344 rats. Toxicol. Pathol. 20, 357–366.

Chan, F.L., Choi, H.L., Underhill, C.B., 1997. Hyaluronan and chondroitin sulfate proteoglycans are colocalized to the ciliary zonule of the rat eye: a histochemical and immunocytochemical study. Histochem. Cell Biol. 187, 289–301.

Cia, D., Bonhomme, B., Azais-Braesco, V., Cluzel, J., Doly, M., 2004. Uptake and esterification of vitamin A by RCS rat retinal pigment epithelial cells in primary culture. Vision Res. 44, 247–255.

Cornell-Bell, A.H., Sullivan, D.A., Allansmith, M.R., 1985. Gender related differences in the morphology of the lacrimal gland. Invest. Ophthalmol. Vis. Sci. 26, 1170–1175.

Cunha-Vaz, J.G., 1997. The blood ocular barriers: past, present and future. Doc. Ophthalmol. 93, 149–157.

D'Cruz, P.M., Yasumura, D., Weir, J., Matthes, M.T., Abderrahim, H., Lavail, M.M., et al., 2000. Mutation of the receptor tyrosine kinase gene Mertk in the retinal dystrophic RCS rat. Hum. Mol. Genet. 9, 645–651.

del Cerro, M., Grover, D., Monjan, A.A., Pfau, C., Dematte, J., 1984. Congenital retinitis in the rat following maternal exposure to lymphocytic choriomeningitis virus. Exp. Eye Res. 38, 313–324.

DiLoreto, D.A., Martzen, M.R., del Cerro, C., Coleman, P.D., del Cerro, M., 1995. Mueller cell changes precede photoreceptor cell degeneration in the age-related retinal degeneration of the Fischer 344 rat. Brain Res. 698, 1–14.

Dorfman, A.L., Joly, S., Hardy, P.l., Chemtob, S., Lachapelle, P., 2009. The effect of oxygen and light on the structure and function of the neonatal rat retina. Doc. Ophthalmol. 118, 37–54.

Draper, C.E., Adeghate, E.A., Lawrence, P.A., Pallot, D.J., Garner, A., Singh, J., 1998. Age-related changes in morphology and secretory responses of male rat lacrimal gland. J. Auton. Nerv. Syst. 69, 173–183.

Draper, C.E., Adeghate, E.A., Singh, J., Pallot, D.J., 1999. Evidence to suggest morphological and physiological alterations of lacrimal gland acini with ageing. Exp. Eye Res. 68, 265–276.

Drenckhahn, D., Jacobi, B., Lullmann-Rauch, R., 1983. Corneal lipidosis in rats treated with amphophilic cationic drugs. Arzneimittelforschung. 33, 827–831.

Dubielzig, R.R., Ketring, K.L., McLellan, G.J., Albert, D.M., 2010. Veterinary Ocular Pathology, a comparative review. Elsevier Ltd, New York, NY.

Duboc, A., Hanoteau, N., Simonutti, M., Rudolf, G., Nehlig, A., Sahel, J.A., et al., 2004. Vigabatrin, the GABA-transaminase inhibitor, damages cone photoreceptors in rats. Ann. Neurol. 55, 695–705.

Dünne, A.A., Steinke, L., Temoortash, A., Kuporpkat, C., Folz, B.J., Werner, J.A., 2004. The lymphatic system of the major head and neck glands in rats. Otolaryngol. Pol. 58, 121–130.

Fabian, R.J., Bond, J.M., Drobeck, H.P., 1967. Induced corneal opacities in the rat. Br. J. Ophthalmol. 51, 124–129.

Ferrara, D., Monteforte, R., Baccari, G.C., Minucci, S., Chieffi, G., 2004. Androgen and estrogen receptors expression in the rat exorbital lacrimal gland in relation to "harderianization". J. Exp. Zool. A Comp. Exp. Biol. 301, 297–306.

Fitch, K.L., Nadakavukaren, M.J., Richardson, A., 1982. Age-related changes in the corneal endothelium of the rat. Exp. Gerontol. 17, 179–183.

Fix, A.S., Horn, J.W., Hall, R.L., Johnson, J.A., Tizzano, J.P., 1995. Progressive retinal toxicity in neonatal rats treated with D, L-2amino-3-phosphonopropionate (D, L-AP3). Vet. Pathol. 32, 521–531.

Fox, D.A., Chu, L. W.-F., 1988. Rods are selectively altered by lead. II. Ultrastructure and quantitative histology. Exp. Eye Res. 46, 613–625.

Gaertner, D.J., Lindsey, J.R., Stevens, J.O., 1988. Cytomegalic changes and "inclusions" in lacrimal glands of laboratory rats. Lab. Anim. Sci. 38, 79–82.

Gelatt, K.N., 2007. Veterinary Ophthalmology. Blackwell Publishing, Ames, IA.

Giknis, M., Clifford, C., 2004. Compilation of Spontaneous Neoplastic Lesions and Survival in Crl:CD (SD) Rats from Control Groups. Charles River Laboratories, Wilmington, MA.

Gregory, A.R., 1973. Ocular edema from carbon monoxide. Aerosp. Med. 44, 567–568.

Gruebbel, M., Hoenerhoff, M., 2010. P-38 Nonneoplastic eye lesions in rats and mice. Toxicol. Pathol. 38, E7–E12.

Gudmundsson, O.G., Sullivan, D.A., Bloch, K.J., Allansmith, M.R., 1985. The ocular secretory immune system of the rat. Exp. Eye Res. 40, 231–238.

Guillet, R., Wyatt, J., Baggs, R.B., Kellogg, C.K., 1988. Anesthetic-induced corneal lesions in developmentally sensitive rats. IOVS. 29, 949–954.

Hanna, C., Jarman, R.V., Keatts, J.G., Duffy, C.E., 1968. Virus induced cataracts. Arch. Ophthalmol. (Chicago). 79, 59–63.

Harkness, J.E., Ridgeway, M.D., 1980. Chromodacryorrhea in laboratory rats *(Rattus norvegicus):* etiologic considerations. Lab. Anim. Sci. 30, 841–844.

Hassel, J.R., Birk, D.E., 2010. The molecular basis of corneal transparency. Exp. Eye Res. 91, 326–335.

Heath, J.E., Rahemtullah, F., Fine, W.D., 2000. Case report: carcinoma of the extraorbital lacrimal gland in a female Fischer 344 rat. Toxicol. Pathol. 28, 824–826.

Heywood, R., 1975. Glaucoma in the rat. Br. Vet. J. 131, 213–221.

Heywood, R., Gopinath, C., 1990. Morphological assessment of visual dysfunction. Toxicol. Pathol. 18, 204–217.

Hubert, M.F., Gillet, J.P., Durand-Cavagna, G., 1994. Spontaneous retinal changes in Sprague–Dawley rats. Lab. Anim. Sci. 44, 561–567.

Hughes, A., 1977. The refractive state of the rat eye. Vision Res. 17, 927–939.

Iandiev, I., Pannicke, T., Reichenbach, A., Wiedemann, P., Bringmann, A., 2007. Diabetes alters the localization of glial aquaporins in rat retina. Neurosci. Lett. 421, 132–236.

Imai, H., Miyata, M., Uga, S., Ishikawa, S., 1983. Retinal degeneration in rats exposed to an organophosphate pesticide (fenthion). Environ. Res. 30, 453–465.

Inagaki, S., Kotani, T., 2002. Examination of the rat eye at the early stage of development with osmium tetroxide. Vet. Ophthalmol. 5, 193–196.

Jammoul, F., Dégardin, J., Pain, D., Gondouin, P., Simonutti, M., Dubus, E., et al., 2010. Taurine deficiency damages photoreceptors and retinal ganglion cells in vigabatrin-treated neonatal rats. Mol. Cell. Neurosci. 43, 414–421.

Janes, R.G., Bounds, G.W., 1955. The blood vessels of the rat's eye. Am. J. Anat. 96, 357–373.

Johnson, T.V., Tomarev, S.I., 2010. Rodent models of glaucoma. Brain Res. Bull. 81, 349–358.

Julien, S., Biesemeier, A., Kokkinou, D., Eibl, O., Schraemeyer, U., 2011. Zinc deficiency leads to lipofuscin accumulation in the retinal pigment epithelium of pigmented rats. PLOS One. 6, 1–8.

Katz, M.L., Robinson Jr., W.G., 1983. Lipofuscin response to the "aging-reversal" drug centrophenoxine in rat retinal pigment epithelium and frontal cortex. J. Gerontol. 38, 525–531.

Kendrey, G., Roe, F.J., 1969. Melanotic lesions of the eye in August hooded rats induced by urethane or *N*-hydroxyurethane given during

the neonatal period: a histopathological study. J. Natl. Cancer Inst. 43, 749–755.
Kobayashi, S., Mukai, N., 1974. Retinoblastoma-like tumors induced by human adenovirus type 12 in rats. Cancer Res. 34, 1646–1651.
Koch, H.R., Fischer, A., Kaufmann, H., 1977. Occurrence of cataracts in spontaneously hypertensive rats. Ophthalmol. Res. 9, 189–193.
Kuno, H., Usui, T., Eydelloth, R.S., Wolf, D.E., 1991. Spontaneous ophthalmic lesions in young Sprague–Dawley rats. J. Vet. Med. Sci. 53, 607–614.
Kuszak, J.R., Zoltoski, R.K., Tiedemann, C.E., 2004. Development of lens sutures. Int. J. Dev. Biol. 48, 889–902.
Lai, Y.-L., 1980. Outward movement of photoreceptor cells in normal rat retina. Invest. Ophthalmol Vis. Sci. 19, 849–856.
Lai, Y.-L., Jacoby, R., Jonas, A.M., 1978. Age-related and light-associated retinal changes in Fischer rats. Invest. Ophthalmol Vis. Sci. 17, 634–638.
Lai, Y.-L., Masuda, K., Mangum, M.D., Lug, R., Macrae, D.W., Fletcher, G., et al., 1982. Subretinal displacement of photoreceptor nuclei in human retina. Exp. Eye Res. 34, 219–228.
Lee, E.W., Render, J.A., Garner, C.D., Brady, A.N., Li, L.C., 1990. Unilateral degeneration of retina and optic nerve in Fischer-344 rats. Vet. Pathol. 27, 439–444.
Lehrer, S., 1981. Blindness increases life span of male rats: pineal effect on longevity. J. Chronic. Dis. 34, 427–429.
Lerman, S., Borkman, R., 1978. Ultraviolet radiation in the aging and cataractous lens. A survey. Acta Ophthalmol. 56, 139–149.
Leuenberger, P.M., 1970. Die Stereo—Ultrastruktur der Cornealoberfläche bei die Ratte. Albrecht Von Graefes Arch. Klin. Exp. Ophthalmol. 180, 182–192.
Leure-duPree, A.E., Mcclain, C.J., 1982. The effect of severe zinc deficiency on the morphology of the rat retinal pigment epithelium. Invest. Ophthalmol. Vis. Sci. 23, 425–434.
Levin, L.A., Nilsson, S.F.E., Ver Hoeve, J., Wu, S.M., Kaufman, P.L., Alm, A., 2011. Adler's Physiology of the Eye. eleventh ed. Elsevier Inc.
Li, D., Sun, F., Wang, K., 2003. Caloric restriction retards age-related changes in rat retina. Biochem. Biophys. Res. Commun. 309, 457–463.
Lin, W.L., Essner, E., 1987. An electron microscopic study of retinal degeneration in Sprague–Dawley rats. Lab. Anim. Sci. 37, 180–186.
Losco, P.E., Troup, C.M., 1988. Corneal dystrophy in Fischer 344 rats. Lab. Anim. Sci. 38, 702–710.
Magnusson, G., Majeed, S., Offer, J.M., 1978. Intraocular melanoma in the rat. Lab. Anim. 12, 249–252.
Mains, J., Tan, L.E., Zhang, T., Young, L., Shi, R., Wilson, C., 2012. Species variation in small molecule components of animal vitreous. Invest. Ophthalmol. Vis. Sci. 53, 4778–4786.
Masland, R.H., 2004. Neuronal cell types. Curr. Biol. 14, R497–R500.
Masland, R.H., 2011. Cell populations of the retina: the Proctor lecture. Invest. Opthalmol. 52, 4581–4591.
Matsusaka, T., 1982. Cytoarchitecture of choroidal melanocytes. Exp. Eye Res. 35, 461–469.
May, P.C., Dean, R.A., Lowe, S.L., Martenyi, F., Sheehan, S.M., Boggs, L.N., et al., 2011. Robust central reduction of amyloid-beta in humans with an orally available, non-peptidic beta-secretase inhibitor. J. Neurosci. 31, 16507–16516.
McAvoy, J.W., 1981. The spatial relationship between presumptive lens and optic vesicle/cup during early eye morphogenesis in the rat. Exp. Eye Res. 33, 447–458.
McMartin, D.N., Sahota, P.S., Gunson, D.E., Han Hus, H., Spaet, R. H., 1992. Neoplasms and related proliferative lesions in control Sprague–Dawley rats from carcinogenicity studies. Historical data and diagnostic considerations. Toxicol. Pathol. 20, 212–225.
Mecklenburg, L., Schraermeyer, U., 2007. An overview on the toxic morphological changes in the retinal pigment epithelium after systemic compound administration. Toxicol. Pathol. 35, 252–267.
Monjan, A.A., Silverstein, A.M., Cole, G.A., 1972. Lymphocytic choriomeningitis virus-induced retinopathy in newborn rats. Invest. Ophthalmol. 11, 850–856.
Morrison, J.C., Fraunfelder, F.W., Milne, S.T., Moore, C.G., 1995. Limbal microvasculature of the rat eye. Invest. Ophthalmol. Vis. Sci. 36, 751–756.
Morrison, J.C., Cepurna Ying Guo, W.O., Johnson, E.C., 2011. Pathophysiology of human glaucomatous optic nerve damage: insights from rodent models of glaucoma. Exp. Eye Res. 93, 156–164.
Morse, E.D., McCann, P.S., 1984. Neuroectoderm of the early embryonic rat eye. Invest. Ophthalmol. Vis. Sci. 25, 899–907.
Nichols, C.W., Yanoff, M., 1969. Dermoid of a rat cornea. Pathol. Vet. 6, 214–216.
Obenberger, H., 1969. Calcification in corneas with alloxan-induced vascularization. Am. J. Ophthalmol. 68, 113–119.
Ogino, H., Ito, M., Matsumoto, K., Yagyu, S., Tsuda, H., Hirono, I., et al., 1993. Retinal degeneration induced by *N*-methyl-*N*-nitrosourea and detection of 7-methyldeoxyguanosine in the rat retina. Toxicol. Pathol. 21, 21–25.
Olliver, F.J., Samuelson, D.A., Brooks, D.E., Lewis, P.A., Kallberg, M. E., Komáromy, A.M., 2004. Comparative morphology of the tapetum lucidum (among selected species). Vet. Ophthalmol. 7, 11–22.
O'Steen, W.K., Brodish, A., 1985. Neuronal damage in the rat retina after chronic stress. Brain Res. 344, 231–239.
O'Steen, W.K., Kraeer, S.L., Shear, C.R., 1978. Extraocular muscle and harderian gland degeneration and regeneration after exposure of rats to continuous fluorescent illumination. Invest. Ophthalmol. Vis. Sci. 17, 847–856.
Patnakar, K.S., Gowreswaramma, P., 1982. Rat cornea in experimental protein deficiency. Ophthalmologica. 185, 46–50.
Payne, A.P., 1994. The harderian gland: a tercentennial review. J. Anat. 185, 1–49.
Peppard, J.V., Montgomery, P.C., 1987. Studies on the origin and composition of IgA in rat tears. Immunology. 62, 193–198.
Percy, D.H., Albert, D.M., 1974. Developmental defects in rats treated postnatally with 5-iododeoxyuridine (IUDR). Teratology. 9, 275–286.
Percy, D.H., Wojcinski, W., Schunk, M.K., 1989. Sequential changes in the harderian and exorbital lacrimal glands in Wistar rats infected with sialodacryoadenitis virus. Vet. Pathol. 26, 238–245.
Pfister, R.R., 1973. The normal corneal epithelium: a scanning electron microscopic study. Invest. Ophthalmol. 12, 654–668.
Price, C.J., Tyl, R.W., Marks, T.A., 1985. Teratologic and postnatal evaluation of aniline hydrochloride in the Fischer 344 rat. Toxicol. Appl. Pharmacol. 77, 465–478.

Puro, D.G., 2012. Retinovascular physiology and pathophysiology: new experimental approach/new insights. Prog. Retin. Eye Res. 31, 258–270.

Qiao, H., Hisatomi, T., Sonoda, K.-H., Kura, S., Sassa, Y., Kinoshita, S., et al., 2005. The characterization of hyalocytes: the origin, phenotype and turnover. Br. J. Ophthalmol. 89, 513–517.

Rao, G.N., 1988. Light intensity-related ophthalmitis of Fischer 344 rats in long-term studies. Lab. Anim. Sci. 38, 497.

Rapp, L.M., Thurn, L.A., Anderson, R.E., 1988. Synergism between environmental lighting and taurine depletion in causing photoreceptor cell degeneration. Exp. Eye Res. 46, 229–238.

Ratnakar, K.S., Gowreswaramma, P., 1982. Rat cornea in experimental protein deficiency. Ophthalmologica. 185, 46–50.

Robinson Jr., W.G., Kuwabara, T., Bieri, J.G., 1980. Deficiencies of vitamins E and A in the rat. Retinal damage and lipofuscin accumulation. Invest. Ophthalmol. Vis. Sci. 19, 1030–1037.

Rogers, J.M., Hurley, L.S., 1987. Effects of zinc deficiency on morphogenesis of the fetal rat eye. Development. 99, 231–238.

Rose, R.C., Gogia, R., Richer, S.P., 1997. Properties of electrochemically active components in mammalian vitreous humor. Exp. Eye Res. 65, 807–812.

Sakai, T., 1981. The mammalian harderian gland: morphology, biochemistry, function and phylogeny. Arch. Histol. Jpn. 44, 299–333.

Sand, A., Schmidt, T.M., Kofuji, P., 2012. Diverse types of ganglion cell photoreceptors in the mammalian retina. Prog. Retin. Eye Res. 31, 287–302.

Schaeppi, U., Krinke, G., FitzGerald, R.E., Ziel, R., 1987. Retinotoxicity of amoscanate in the albino rat. Conc. Toxicol. 4, 179–182.

Shearer, T.R., Ma, H., Fukiage, C., Azuma, M., 1997. Selenite nuclear cataract: review of the model. Mol. Vis. 3, 8.

Sheline, C.T., Zhou, Y., Bai, S., 2010. Light-induced photoreceptor and RPE degeneration involve zinc toxicity and are attenuated by pyruvate, nicotinamide, or cyclic light. Mol. Vis. 16, 2639–2652.

Shibuya, K., Tajima, N., Nunoya, T., 1998. Optic nerve Dysplasia associated with meningeal defect in Sprague–Dawley rats. Vet. Pathol. 35, 323–329.

Shinowara, N.L., London, E.D., Rapoport, S.I., 1982. Changes in retinal morphology and glucose utilization in aging albino rats. Exp. Eye Res. 34, 517–530.

Smith, R.S., Hoffman, H., Cisar, C., 1969. Congenital cataract in the rat. Arch. Ophthalmol. 81, 259–263.

Spencer, W.H., 1986. Ophthalmic Pathology, vol. 3. Saunders, Philadelphia, PA.

Steinhagen, W.H., Swenberg, J.A., Barrow, C.S., 1982. Acute inhalation toxicity and sensory irritation of dimethylamine. Am. Ind. Hyg. Assoc. J. 43, 411–417.

Tanaka, K., Inagaki, S., Ohmori, R., Kuno, H., Matsumoto, H., Usui, T., 1993. Focal chorioretinal atrophy in rats. J. Toxicol. Pathol. 93, 205–211.

Taniguchi, H., Kitaoka, T., Gong, H., Amemiya, T., 1999. Apoptosis of the hyaloid artery in the rat eye. Ann. Anat. 181, 555–560.

Taradach, C., Greaves, P., 1983. Spontaneous eye lesions in laboratory animals: incidence in relation to age. CRC Crit. Rev. Toxicol. 12, 121–147.

ten Tusscher, M.P., et al., 1989a. The allocation of nerve fibres to the anterior eye segment and peripheral ganglia of rats. I. The sensory innervation. Brain Res. 494, 95–104.

ten Tusscher, M.P., et al., 1989b. The allocation of nerve fibres to the anterior eye segment and peripheral ganglia of rats. II. The sympathetic innervation. Brain Res. 494, 105–113.

Theocharis, D.A., Skandalis, S.S., Noulas, A.V., Papageorgakopoulou, N., Theocharis, A.D., Karamanos, N.K., 2008. Hyaluronan and chondroitin sulfate proteoglycans in the supramolecular organization of the mammalian vitreous body. Connect. Tissue Res. 49, 124–128.

Thompson, D.A., Gal, A., 2003. Vitamin A metabolism in the retinal pigment epithelium: genes, mutations, and diseases. Prog. Retin. Eye Res. 22, 683–703.

Tso, M.O.M., Zhang, C., Abler, A.S., Chang, C.J., Wong, F., Chang, G.Q., et al., 1994. Apoptosis leads to photoreceptor degeneration in inherited retinal dystrophy of RCS rats. Invest. Ophthalmol. Vis. Sci. 35, 2693–2699.

Ugarte, M., Osborne, N.N., 2001. Zinc in the retina. Prog. Neurobiol. 64, 219–249.

Ugarte, M., Grime, G.W., Lord, G., Geraki, K., Collingwood, J.F., Finnegan, M.E., et al., 2012. Concentration of various trace elements in the rat retina and their distribution in different structures. Metallomics. 4, 1245–1254.

Ulrich, R., Yuwiler, A., Geller, E., Wetterberg, L., 1974. Effects of sex hormones and environmental lighting on rat harderian gland porphyrin. J. Endocrinol. 63, 99–102.

Valamanesh, F., Torriglia, A., Savoldelli, M., Gandolphe, C., Jeanny, J.-C., BenEzra, D., et al., 2007. Glucocorticoids induce retinal toxicity through mechanisms mainly associated with paraptosis. Mol. Vis. 13, 1746–1757.

de Vera Mudry, M.C., Kronenberg, S., Komatsu, S., Aguirre, G.D., 2013. Blinded by the light: retinal phototoxicity in the context of safety studies.. Toxicol. Pathol. 41, 813–825.

von Voigtlander, P.F., Kolaja, G.J., Block, E.M., 1982. Corneal lesions induced by antidepressants: a selective effect upon young Fischer 344 rats. J. Pharmacol. Exp. Ther. 222, 282–286.

Wagner, N., Kanai, A., Harrington, J.S., Kaufman, H.E., Nakamoto, T., 1983. Cataract formation in newborn rats from feeding a liquid protein diet during gestation. Exp. Eye Res. 37, 129–138.

Wang, J.-S., Kefalov, V.J., 2011. The cone-specific visual cycle. Prog. Retin. Eye Res. 30, 115–128.

Wetterberg, L., Geller, E., Yuwiler, A., 1970. Harderian gland: an extraretinal photoreceptor influencing the pineal gland in neonatal rats? Science. 167, 884–885.

Wilcock, B.P., 2007. Pathology of Domestic Animals, vol. 1. Elsevier, Philadelphia, PA.

Williams, D.L., 2002. Ocular disease in rats: a review. Vet. Ophthalmol. 5, 183–191.

Wolf, N.S., Li, Y., Pendergrass, W., Schmeider, C., Turturro, A., 2000. Normal mouse and rat strains as models for age-related cataract and the effect of caloric restriction on its development. Exp. Eye Res. 70, 683–692.

Woolf, D., 1956. A comparative cytological study of the ciliary muscle. Anat. Rec. 124, 145–163.

Yoshizawa, K., Sasaki, T., Uehara, N., Kuro, M., Kimurai, A., Kinoshita, Y., et al., 2012. *N*-ethyl-*N*-nitrosourea induces retinal photoreceptor damage in adult rats. J. Toxicol. Pathol. 25, 27–35.

Young, C., Hill, A., 1974. Conjunctivitis in a colony of rats. Lab. Anim. 8, 301–304.

Young, C., Festing, M.F.W., Barnett, K.C., 1974. Buphthalmos (congenital glaucoma) in the rat. Lab. Anim. 8, 21–31.

Yu, C.Q., Schwab, I.R., Dubielzig, R.R., 2009. Feeding the vertebrate retina from Cambrian to the Tertiary. J. Zoo. 278, 259–269.

Zeiss, C.J., 2010. Review paper: animals as models of age-related macular degeneration: an imperfect measure of the truth. Vet. Pathol. 47, 396–413.

Zwicker, G.M., Fikes, J.D., Thruman, J.D., Rogers, B.A., Bucci, T.J., 1997. Spontaneous proliferative melanocytic lesions in ad libitum and forty percent dietary restriction fed Brown Norway and F1BNF rats of Brown Norway × Fisher 344 mating. The 16th International Symposium of the Society of Toxicologic Pathologists.